Journal of Sedimentary Environments (2022) 7:471–499
https://doi.org/10.1007/s43217-022-00106-6

ORIGINAL ARTICLE

Provenance composition, paleo-weathering and tectonic setting of Himalayan foreland basin sediments, Kumaun Sub-Himalaya, India

Dinesh S. Chauhan[1] · Ritu Chauhan[1] · Bhupender Singh[1]

Received: 17 December 2021 / Revised: 9 May 2022 / Accepted: 12 May 2022 / Published online: 4 June 2022

Abstract

Clastic rocks of foreland basin from Nandhaur Sanctuary area, Kumaun Sub-Himalaya were studied to interpret their lithological composition, provenance, source area weathering characteristics and tectonic setting. Detailed geochemical investigation on 33 mudstone and petrographic study of 25 sandstone samples have been carried out. Sandstones are classified as quartz-arenite to sublith-arenite; lithic to subarkosic arenite and lithic to arkosic greywacke using detrital mode analysis. Chemically, mudstone is identified as greywacke to lithic-arenite and also straddles between shale and wacke with a few in lithic-arenite field. CIA values vary from 55.8 to 78.7 for Lower Siwalik, 53–78.3 for Middle Siwalik and, 58.8–81.7 for Upper Siwalik sediments. These results suggest that differential weathering conditions acted upon the sediment provenance: under steady to non-steady-state, variable climatic conditions, and Cenozoic tectonic uplifting along Himalayan thrusts. Chemical data in Al_2O_3-CaO-Na_2O-K_2O (A-CN-K) plot depart from the granite-granodiorite field towards the illite-muscovite indicating weathering trend in provenance. Chemically, mudstone bears the signature of Passive Margin tectonic setting of deposition which is inherited from the source rock. High field strength element (HFSE) and Rare Earth Element (REE) content of mudstone support the felsic upper crustal material as source, whereas transition elements advocate minor contribution from mafic rocks. Chondrite normalized high Light REE (LREE)/ Heavy REE (HREE) ratio (11.15–15.11), sloping LREE and near-flat HREE, negative Eu anomaly (Eu/Eu* = 0.6–0.88) indicate the evolved upper crustal material as the prominent source. The trace element ratio in mudstone; La/Sc (0.71–5.86), Cr/Th (2.42–9.50), Th/Co (0.07–0.95), and La/Co (0.15–2.31), supports the sediment derivation from felsic sources however Th/Co values indicate the mixed source rocks. The geochemistry of mudstone shows affinity with the rocks of high-grade Higher Himalaya and low-grade Lesser Himalaya and is a useful proxy for understanding the various tectonic and paleo-climatic conditions that prevailed during the evolution of Himalayan Foreland Basin.

Keywords Siwalik · Sedimentary geochemistry · Tectonic setting · Provenance · Weathering · Kumaun Himalaya · Nainital

1 Introduction

The Foreland basin is a result and characteristic of collision-related mountainous belts, often developed as an elongated trough along the mountainous fold and thrust belt. It is often sandwiched on the continental crust with a contractional orogenic belt on one side and an adjacent craton on another with enormous potential of sediment accommodation (DeCelles & Giles, 1996). The basin fill receives the sediments dominantly from the exhuming fold and thrust belt with a minor contribution from the cratonic part (DeCelles & Hertel, 1989; Dickinson & Suczek, 1979; Sawant et al., 2017; Schwab, 1986). Thus, the characterization of the sediments, deposited in the foreland basin offer the opportunity to unravel the history of the exhumation and source categorization in the uplifting fold and thrust belt. The nature, size and thickness of the sediments being deposited in the foreland basin depends on the actual site of deposition relative to the advancing fold and thrust system and flexure bending of the subducting portion.

In addition to the petrographic studies of clastic rocks to demarcate the tectonic setting of basin evolution and characterization of provenance, their geochemistry is widely

Communicated by M. V. Alves Martins

✉ Dinesh S. Chauhan
dinesh_geo@rediffmail.com

[1] Geological Survey of India, Bhopalpani Grant, Dehradun, India

used to interpret the depositional setting, provenance, exhumation records and climate-tectonic interaction (Awasthi, 2017; Bhakuni et al., 2012; Huyghe et al., 2001; Khan et al., 2019, 2020; Mandal et al., 2018; Roddaz et al., 2005; Roser & Korsch, 1986; Sawant et al., 2017; Van Der Beek et al., 2006; Wesnousky et al., 1999). The Himalayan foreland basin is filled with hundreds to thousands of meter thicknesses of sediments that have preserved the records of Cenozoic continental collision between Indian and Eurasian Plates. These records involve the signature of exhumation and upliftment from beginning to termination stage of collision and post-collision. The spatial and temporal distribution of sediments, their geochemical records and isotopic signatures can be used to demarcate the complete exhumation history and related foreland/hinterland propagated thrust belt. Thus, the whole-rock geochemical analysis of the sandstone-mudstone-shale sequence in a foreland basin can be used as a proxy to understand the evolution of the mountain belt and tectonics involved (DeCelles et al., 1998; Ghosh & Kumar, 2000; Hussain & Bharali, 2019; Mandal et al., 2018; Najman & Garzanti, 2000; Van Der Beek et al., 2006).

The chemistry of both flysch and molasse sediments is a significant tool to address their source characteristics, as well as the weathering of the source rock, climatic conditions and tectonic setting of deposition. Major oxide, trace and REE contents of the sedimentary rocks are important contributors to characterize the provenance and tectonic setting. The major oxide values of the mudstone provide crucial information on alteration indices to identify the quantitative and qualitative characterization of paleo-weathering conditions. Trace element concentrations in the sediments (clay-rich) are useful proxy to address their source characteristics as well as the tectonic setting of deposition (André et al., 1986; Bhatia & Crook, 1986; Bhatia & Taylor, 1981; McLennan et al., 1980). The immobile nature of some trace elements, and thus their constant/ near-constant ratio makes them excellent contributors in source recognition (Rollinson, 1993) as these elements are associated with a terrigenous component of sediments. The rare earth elements (REE) are thought to be immobile and their both relative and absolute concentration in the sedimentary rocks are not altered during weathering, transportation and depositional processes, because transportation is governed primarily by mechanical rather than chemical changes, preserving the original signatures of source region lithologies and depositional processes of clastic sedimentary rocks (Nance & Taylor, 1976; McLennan, 1989). The provenance, source characteristics, tectonic control along with influences of sedimentary processes has been well studied using REE concentration in sedimentary rocks (Bhatia, 1985; McLennan, 1989). The present study focuses on the geochemistry of the Siwalik mudstone from east of Nandhaur River till Sarra gad/Kalaunia gad in Kumaun Sub-Himalaya to identify the provenance, its chemical weathering, climatic conditions and tectonic setting of deposition. Mudstone is given more preference than sandstone, conglomerate, since the fine clastic sediments carry a very precise rock composition signature, are better mixed, resulting in a more homogenous mixture than coarser sediment fractions (Najman, 2006). To date, few records on sedimentary geochemistry of Siwalik sediments are available from Himachal Himalaya (Ali et al., 2021; Ranjan & Banerjee, 2009; Sinha et al., 2007, 2008), from Central Himalaya in Nepal (DeCelles et al., 1998; Najman & Garzanti, 2000; Ulak et al., 2008) and from Northeast area (Hussain & Bharali, 2019; Roy & Roser, 2013; Sawant et al., 2017). No comprehensive geochemical investigation on mudstone is available on Siwalik sediments in Kumaun Sub-Himalaya. Mandal et al. (2018) studied the isotopic and geochemical signature of Siwalik sandstone in Dehradun re-entrant. The Nandhaur Sanctuary area also lacks the detailed geological investigation in Siwalik Group on regional scale. For this purpose, the geological mapping has been carried out on the 1:25,000 scales recording the lithological variation, petrography and geochemical analysis in almost 225 km^2 areas. Thus, the work presents the first-hand detailed geological mapping of the area. The work portrays the sandstone petrography and mudstone geochemistry to establish the source region characteristics, temporal variation in suppliers and role of tectonics in the chemical signature of sediments in this segment of the Siwalik Range.

2 Geological setting

The Himalaya is the result of crustal-scale geodynamic processes involving subduction of oceanic plate followed by the Cenozoic collision between the Indian and Eurasian plates (Gansser, 1964; Heim & Gansser, 1939; Thakur, 1992). The collision resulted in the upheaval of the Proterozoic-Early Cenozoic rock sequences and the development of the largest and the youngest foreland basin on the Indian subcontinent (Valdiya, 1980; Yin, 2006). The development of global scale tectonic boundaries in the Himalaya divides it into various segments. From north to south these are Trans Himalaya, Tethyan sequence, Higher Himalaya, Lesser Himalaya and Siwalik sediments (Fig. 1a). The Trans-Himalaya in the north of Indus-Tsang Po Suture zone (ITSZ) comprises the Calc alkaline Laddakh batholith sequence of Upper Cretaceous to Eocene age and Tso-Morari dome with eclogites and marine origin metasedimentary sequence (LeFort, 1996). The Cambrian to Eocene age fossiliferous sedimentary rocks, known as Tethyan sedimentary sequence; is exposed in the south of ITSZ. These rocks abut the Higher Himalaya in south along normal fault contact known as South Tibet Detachment (STD), shown in Fig. 1a (Burchfiel et al., 1992; Burg et al., 1984). It is also proposed that

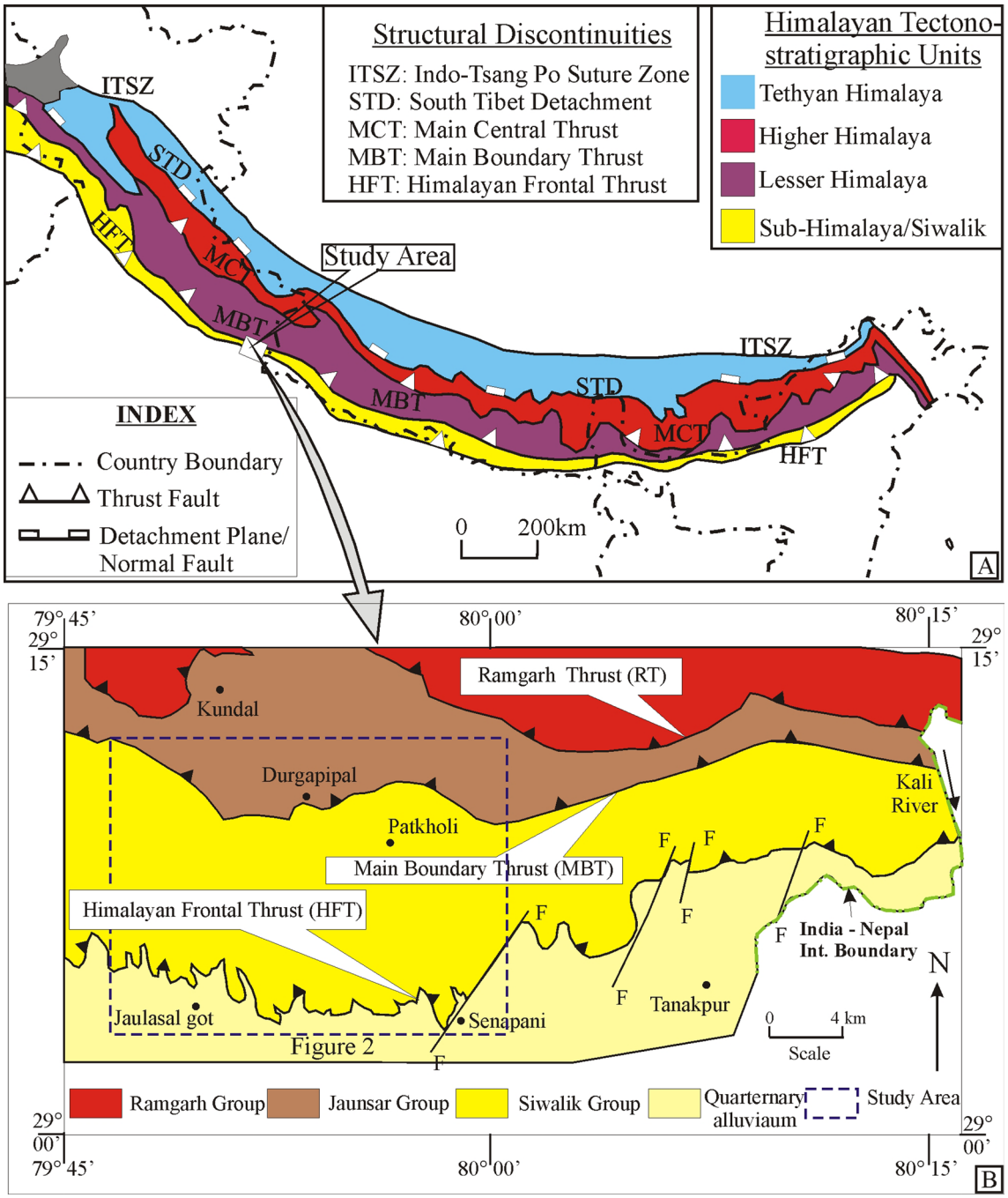

Fig. 1 **a** Geological Map of the Himalaya showing major tectonic boundaries and location of the study area (after Gansser, 1964), **b** Geological map of the part of Kumaun Lesser Himalaya showing present study area (Map compiled after Raina & Dungrakoti, 1965; Kumar & Kothiyal, 1993; Saxena, 1975, 1978; Das et al., 1974 and; Singh & Kothiyal, 1997)

Higher Himalayan rocks form the basement for the Tethyan sediment with the normal order of metamorphic grade (LeFort, 1975). The Higher Himalaya comprises catazonal metamorphics of granite gneiss, quartzite, pelitic schists, calc silicates and Paleozoic and Cenozoic granitoid assemblage up to upper amphibolite facies. The Higher Himalaya is thrust over the Lesser Himalaya along south directed thrust system known as Main Central Thrust (MCT) (Heim & Gansser, 1939; Searle et al., 2008; Thakur, 1992; Valdiya, 1980). The MCT developed as a consequence to accommodate the collision-related crustal shortening during the Middle to Late Miocene age (Najman & Garzanti, 2000; Yin, 2006). The Lesser Himalaya comprises low-grade unfossiliferous metasedimentary sequence of Proterozoic

to Lower Paleozoic age. In the south, the Lesser Himalayan rocks are thrust over the Paleogene–Neogene sequence of Sub-Himalaya along Main Boundary Thrust (MBT) (DeCelles et al., 2001; DiPietro & Pogue, 2004; Fuchs & Linner, 1995; Gansser, 1964; Heim & Gansser, 1939). The Neogene sediments, also known as Siwalik Group, comprise molasse sediments of Middle Miocene to Lower Pleistocene age, deposited in the foreland basin. The rocks of Siwalik Group are thrust over the Indo-Gangetic Plain, the present-day active foreland basin (Fig. 1b), along Main Frontal Thrust (MFT) (Jayangondaperumal et al., 2018; Thakur, 2013). The Indo-Gangetic Plain comprises Quaternary age unconsolidated sediments, further classified into Older and Newer Alluvium.

3 Study area

The study area forms a part of Nandhaur Sanctuary between Nandhaur River in the west and Kalaunia gad in the east (Fig. 2). The Siwalik Group in the study area comprises Nahan (Lower Siwalik), Dewal and Mohargarh (Middle Siwalik) and Pinjor formations Upper Siwalik. These rocks are exposed in the Saj gad—Kalaunia gad section and many north–south trending tributaries. This litho-package is thrust over Quaternary sediments of Indo-Gangetic plains along Himalayan Frontal Thrust (HFT). In the north, the rocks of Siwalik Group are under thrust with Nagthat Formation of Jaunsar Group of Lesser Himalaya and partly by Amritpur granite along Main Boundary Thrust (MBT). Within the Siwalik, the rocks of Nahan Formation are thrust over Pinjor Formation along Lugad Thrust in the northern sector. (Das et al., 1974; Kumar and Kothiyal, 1993; Raina and Dungrakoti, 1965; Saxena, 1975, 1978; Singh & Kothiyal, 1997).

4 Materials and methods

From the various mudstone-sandstone association of Lower to Upper Siwalik rocks, the 33 mudstone samples (12 for Lower Siwalik; 16 for Middle Siwalik and 05 for Upper Siwalik) for geochemistry and 25 sandstone-mudstone samples (06 for Lower Siwalik; 11 for Middle Siwalik and 08 for Upper Siwalik) for petrography were collected. The sample abbreviations and related stratigraphic levels of each sample are shown in the Fig. 2 and details of each sample along with chemical analysis are given in

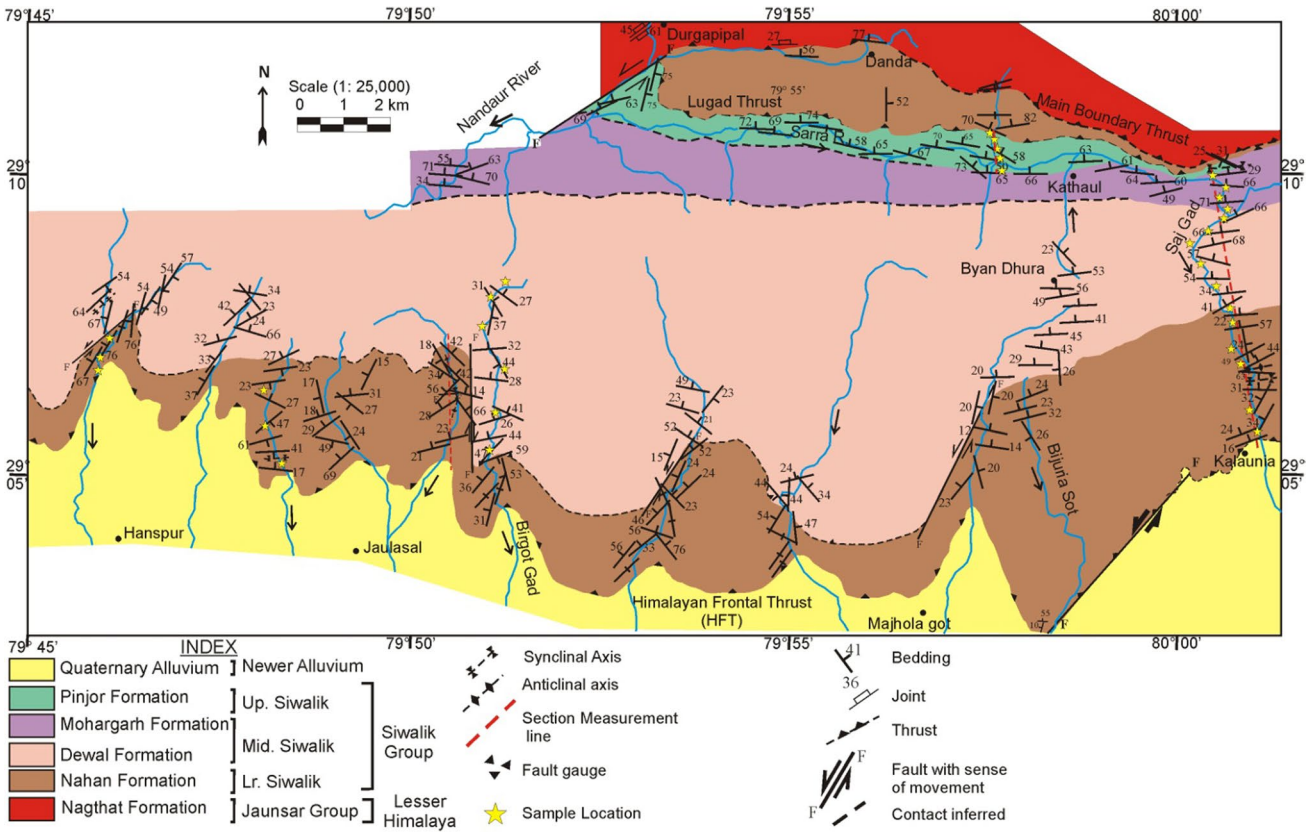

Fig. 2 Geological map of the Siwalik Group in part of Nainital and Champawat districts, Uttarakhand

Table 1 Major Oxide composition of the Siwalik mudstone samples from Nandhaur Sanctuary area (all values of oxide in wt%)

Sample No	Formation	Long (E) DMS	Lat (N) DMS	SiO_2	Al_2O_3	Fe_2O_3	CaO	MgO	Na_2O	K_2O	MnO	TiO_2	P_2O_5	LOI	K_2O/Na_2O	SiO_2/Al_2O_3	TiO_2/Al_2O_3	K_2O/Al_2O_3	Al_2O_3/TiO_2	CIA	PIA	ICV
01A/REE/STM	Lower	79 45 57	29 06 43	–	–	–	–	–	–	–	–	–	–	–	–	–	–	–	–	–	–	–
03/REE/STM	Lower	79 45 57	29 06 57	–	–	–	–	–	–	–	–	–	–	–	–	–	–	–	–	–	–	–
07/REE/STM	Lower	79 46 04	29 07 15	–	–	–	–	–	–	–	–	–	–	–	–	–	–	–	–	–	–	–
07A/REE/STM	Lower	79 48 18	29 05 20	–	–	–	–	–	–	–	–	–	–	–	–	–	–	–	–	–	–	–
14/REE/STM	Lower	80.01 04	29 05 49	67.44	18.68	4.77	0.18	0.85	0.33	4.03	0.03	0.76	0.07	3.46	12.21	3.61	0.04	0.22	24.58	78.7	95.3	0.59
15/REE/STM	Lower	79 48 14	29 06 25	61.31	17.53	8.16	1.2	1.19	0.18	3.75	0.09	0.65	0.15	5.35	20.83	3.50	0.04	0.21	26.97	73.9	86.4	0.87
17/REE/STM	Lower	79 48 25	29 06 46	57.01	17.37	6.91	5.33	1.1	0.31	3.46	0.17	0.55	0.08	8.14	11.16	3.28	0.03	0.20	31.58	55.8	57.6	1.03
18/REE/STM	Lower	80 01 12	29 05 42	65.31	19.37	5.53	0.37	1.11	0.3	4.06	0.07	0.65	0.09	3.19	13.53	3.37	0.03	0.21	29.80	78.4	94	0.62
33/REE/STM	Lower	80 01 04	29 06 03	75.25	14.54	3.7	0.24	1.08	0.47	3.68	0.02	0.62	0.07	2.38	7.83	5.18	0.04	0.25	23.45	74.3	91	0.67
34/REE/STM	Lower	80 36 57	29 06 50	69.26	13.76	4.91	1.29	1.04	0.29	3.54	0.03	0.57	0.07	2.89	12.21	5.03	0.04	0.26	24.14	68	78.9	0.85
35/REE/STM	Lower	80 00 50	29 07 04	69.35	14.53	6.16	0.5	1.6	0.47	3.38	0.03	0.63	0.03	4.03	7.19	4.77	0.04	0.23	23.06	73.4	87.1	0.88
36/REE/STM	Lower	80 00 50	29 07 33	70.18	14.87	4.91	0.65	1.31	0.31	3.66	0.03	0.65	0.03	5.20	11.81	4.72	0.04	0.25	22.88	72.7	87.1	0.77
08/REE/STM	Middle	79 03 28	29 05 27	82.95	8.42	2.46	0.17	1.96	0.37	1.49	0.02	0.45	0.06	2.56	4.03	9.85	0.05	0.18	18.71	77.9	89.8	0.82
09/REE/STM	Middle	79 03 03	29 06 07	83.55	7.76	1.92	0.15	1.44	0.5	1.46	0.02	0.59	0.08	2.22	2.92	10.77	0.08	0.19	13.15	75.8	87.2	0.78
10/REE/STM	Middle	79 51 10	29 06 46	81.3	7.86	1.65	1.99	1.35	0.45	1.33	0.02	0.53	0.08	3.77	2.96	10.34	0.07	0.17	14.83	58.4	60.6	0.93
11/REE/STM	Middle	79 51 00	29 07 22	86.24	4.84	1.01	1.57	0.91	0.52	0.58	0.03	0.28	0.02	2.37	1.12	17.82	0.06	0.12	17.29	53	53.5	1.01
11a/REE/STM	Middle	79 51 03	29 07 55	69.08	17.84	6.45	0.15	1.15	0.47	3.5	0.02	0.66	0.04	2.58	7.45	3.87	0.04	0.20	27.03	79	93.7	0.70
12/REE/STM	Middle	79 51 21	29 08 13	65.38	17.07	6.19	0.6	0.81	0.22	4.24	0.05	0.65	0.18	4.10	19.27	3.83	0.04	0.25	26.26	75.3	92.4	0.75
13/REE/STM	Middle	80 00 50	29 07 48	61.85	17.62	8.21	0.13	1.01	0.31	3.9	0.03	0.6	0.04	4.70	12.58	3.51	0.03	0.22	29.37	78.3	95.4	0.81
16/REE/STM	Middle	80 00 39	29 08 09	66.37	17.63	5.76	0.33	1.08	0.24	3.86	0.02	0.65	0.08	4.44	16.08	3.76	0.04	0.22	27.12	78	94.4	0.68

Table 1 (continued)

Sample No	Formation	Long (E) DMS	Lat (N) DMS	SiO_2	Al_2O_3	Fe_2O_3	CaO	MgO	Na_2O	K_2O	MnO	TiO_2	P_2O_5	LOI	K_2O/Na_2O	SiO_2/Al_2O_3	TiO_2/Al_2O_3	K_2O/Al_2O_3	Al_2O_3/TiO_2	CIA	PIA	ICV
25a/REE/STM	Middle	80 00 25	29 08 31	73.49	13.14	4.51	0.61	1.62	0.27	2.76	0.05	0.61	0.04	3.98	10.22	5.59	0.05	0.21	21.54	74.7	87.4	0.79
26/REE/STM	Middle	80 00 18	29 08 52	81.22	12.1	3.35	0.34	1.31	0.33	2.53	0.02	0.61	0.03	0.68	7.67	6.71	0.05	0.21	19.84	76	89.6	0.70
29/REE/STM	Middle	80 00 32	29 09 07	63.31	12.99	4.66	4.83	1.44	0.49	3.4	0.04	0.51	0.1	8.33	6.94	4.87	0.04	0.26	25.47	49.9	49.9	1.18
30/REE/STM	Middle	80 00 46	29 09 14	59.15	19.28	8.68	0.41	0.8	0.27	4.17	0.04	0.61	0.04	4.77	15.44	3.07	0.03	0.22	31.61	77.5	93.1	0.78
30a/REE/STM	Middle	80 00 46	29 09 28	74.21	12.08	5.23	1.19	2.32	0.8	2.83	0.04	0.64	0.07	2.55	3.54	6.14	0.05	0.23	18.88	65.5	73.1	1.08
31/REE/STM	Middle	80 00 39	29 09 39	72.79	13.17	4.88	0.29	1.96	0.67	3.2	0.03	0.65	0.05	3.57	4.78	5.53	0.05	0.24	20.26	72.6	86.5	0.89
32/REE/STM	Middle	80 00 46	29 09 50	68.87	15.59	5.79	0.24	1.29	0.45	3.68	0.03	0.65	0.05	3.82	8.18	4.42	0.04	0.24	23.98	75.6	91.7	0.78
37/REE/STM	Middle	80 00 36	29 09 57	73.92	11.97	4.43	1.1	1.92	0.48	2.57	0.05	0.61	0.07	4.49	5.35	6.18	0.05	0.21	19.62	68.9	77.8	0.93
19/REE/STM	Upper	79 57 50	29 10 04	62.24	18.04	6.22	1.06	0.92	0.2	4.13	0.04	0.63	0.11	7.02	20.65	3.45	0.03	0.23	28.63	73.6	87.2	0.73
20/REE/STM	Upper	79 57 47	29 10 15	74.76	11.99	3.77	0.89	1.35	0.43	2.85	0.04	0.49	0.1	4.68	6.63	6.24	0.04	0.24	24.47	69.9	81	0.82
21/REE/STM	Upper	79 57 43	29 10 26	65.39	17.23	3.83	0.55	1.5	0.15	3.48	0.03	0.75	0.06	8.07	23.20	3.80	0.04	0.20	22.97	78	92.4	0.60
22/REE/STM	Upper	79 57 43	29 10 33	63.64	19.27	6.74	0.38	0.73	0.12	3.35	0.15	0.73	0.08	6.16	27.92	3.30	0.04	0.17	26.40	81.7	95.7	0.63
23/REE/STM	Upper	79 57 39	29 10 44	62.78	15.7	4.9	4.29	1.42	0.2	2.89	0.06	0.6	0.11	8.17	14.45	4.00	0.04	0.18	26.17	58.8	61.5	0.91

Table 2 Trace element composition of the Siwalik mudstone samples from Nandhaur Sanctuary area (all values of trace elements in mg kg^{-1})

Sample No	Ba	Co	Cr	Cu	Ga	Nb	Ni	Pb	Rb	Sc	Sr	Th	V	Y	Zn	Zr	U	Cr/Th	Zr/Sc	Th/Sc	Cr/Ni
14/REE/STM	828	125	94	40	22	20	55	46	175	17	59	23	162	81	94	357	5.75	4.09	21.00	1.35	1.71
15/REE/STM	735	84	152	28	22	18	37	26	132	20	76	16	201	35	71	215	4.37	9.50	10.75	0.80	4.11
17/REE/STM	530	35	66	23	22	16	29	22	140	19	36	16	101	32	78	185	3.96	4.13	9.74	0.84	2.28
18/REE/STM	993	47	95	30	25	18	46	18	174	17	45	17	154	34	100	208	3.77	5.59	12.24	1.00	2.07
33/REE/STM	758	64	73	30	17	14	28	21	175	15	36	19	88	24	78	246	2.08	3.84	16.40	1.27	2.61
34/REE/STM	670	31	68	23	17	14	26	29	145	16	47	18	86	28	69	237	2.32	3.78	14.81	1.13	2.62
35/REE/STM	814	45	68	26	20	14	31	21	149	20	46	18	109	29	60	192	2.05	3.78	9.60	0.90	2.19
36/REE/STM	649	30	74	21	21	18	23	22	180	10	79	17	75	27	62	242	2.78	4.35	24.20	1.70	3.22
08/REE/STM	615	102	60	16	8	9	18	17	70	17	18	NA	53	20	40	126	2.7	–	7.41	–	3.33
09/REE/STM	745	126	51	18	9	9	11	18	67	17	21	NA	46	27	37	333	3.67	–	19.59	–	4.64
10/REE/STM	422	77	46	10	8	9	6	18	65	17	42	NA	34	24	27	290	3.15	–	17.06	–	7.67
11/REE/STM	1155	103	37	20	<5	5	5	23	36	21	38	NA	<20	13	29	124	1.81	–	5.90	–	7.40
11a/REE/STM	963	33	87	32	22	16	45	22	154	18	78	NA	136	37	82	195	4.09	–	10.83	–	1.93
12/REE/STM	788	271	100	32	20	17	48	25	191	16	59	18	133	34	90	221	3.41	5.56	13.81	1.13	2.08
13/REE/STM	1085	36	83	26	22	16	43	29	154	18	71	14	139	35	85	175	2.59	5.93	9.72	0.78	1.93
16/REE/STM	756	55	85	28	20	16	30	29	158	16	47	16	109	30	71	245	3.37	5.31	15.31	1.00	2.83
25a/REE/STM	737	117	58	17	16	13	23	21	132	15	49	18	83	30	49	221	3.04	3.22	14.73	1.20	2.52
26/REE/STM	726	98	61	22	14	12	21	23	123	16	34	18	72	29	49	248	2.80	3.39	15.50	1.13	2.90
29/REE/STM	447	107	53	20	19	13	23	24	154	18	96	16	66	23	60	196	2.40	3.31	10.89	0.89	2.30
30/REE/STM	922	22	101	34	25	18	53	30	170	20	65	16	176	34	92	153	2.44	6.31	7.65	0.80	1.91
30a/REE/STM	745	71	46	21	17	13	27	22	118	20	48	19	88	31	51	275	2.58	2.42	13.75	0.95	1.70
31/REE/STM	849	67	52	20	18	13	22	23	157	17	56	20	88	30	64	244	2.71	2.60	14.35	1.18	2.36
32/REE/STM	815	54	71	31	20	15	33	25	174	18	55	18	115	31	67	239	2.23	3.94	13.28	1.00	2.15
37/REE/STM	457	28	65	17	14	17	27	18	120	9	71	16	61	28	63	235	2.94	4.06	26.11	1.78	2.41
19/REE/STM	582	20	75	29	24	16	24	19	184	16	60	19	115	39	79	192	3.40	3.95	12.00	1.19	3.13
20/REE/STM	383	89	49	17	14	15	14	20	158	8	53	16	59	31	51	247	3.14	3.06	30.88	2.00	3.50
21/REE/STM	554	69	97	29	23	21	51	31	173	11	50	20	109	35	89	203	5.95	4.85	18.45	1.82	1.90
22/REE/STM	849	65	81	20	22	17	38	24	146	19	37	16	151	37	78	197	3.96	5.06	10.37	0.84	2.13
23/REE/STM	510	108	81	21	18	13	34	23	131	16	58	12	87	28	59	189	2.87	6.75	11.81	0.75	2.38

NA Not analyzed

Table 1, 2, 3. The mudstone samples were carefully collected avoiding any pedogenetic modifications and were analyzed for the major oxide, trace elements and REE content. All the analysis was performed in the Geological Survey of India Northern Region Labs.

The whole rock chemical composition including major oxides and trace elements were analyzed using *Bruker* Make S8 Tiger X-Ray Fluorescence (XRF). The pallet method was applied for the chemical analysis. The detection limit was 0.1% and 1.00 mg/l for major and trace elements, respectively. GSD10 with known element concentrations was used as standard reference material. The standard was analyzed after each batch of 20 samples for accuracy and duplicate samples after each batch of 10 samples was analyzed for repeatability. The accuracy of the measurement during the entire analysis remains ± 3% with precision of ± 5%. *Varian* make Inductively Coupled Plasma Mass-Spectrometer (ICP MS) instrument was used for the Rare Earth Element analysis with quantification limit in the range of 0.1 to 1.00 mg kg-1. The XRF and ICP-MS analysis were carried out as per procedure given in Lucas-Tooth and Pyne (1964), Rollinson (1993) and Khanna et al., (2009).

The modal analysis was performed on the Olympus BX51 TRF Petrological Microscope following the traditional method for counting the different detrital grains (Basu et al. 1975; Folk, 1974; Mack and Suttner 1977). The different detrital minerals and lithic fragments were identified and counted separately as monocrystalline quartz (Qm), polycrystalline quartz (Qp), K-feldspar (kfs), plagioclase (pl), biotite (bt), muscovite (mus), and lithic fragments individually. The Qm + Qp = Qt; kfs + pl + granite gneiss = Ft and all finer rock fragments are taken together as Rf (after Folk, 1980), whereas these parameters were recalculated keeping in mind the size fraction of these ingredients following the procedure of Dickinson (1985) to present the quartz–feldspar–lithic fragment (Q–F–L) plot. Nearly 250–300 detrital

Table 3 REE composition of the Siwalik mudstone samples from Nandhaur Sanctuary area (all values are in mg kg^{-1})

Sample No	La	Ce	Pr	Nd	Sm	Eu	Gd	Tb	Dy	Ho	Er	Tm	Yb	Lu	Eu/Eu*	La_N/Sm_N	Gd_N/Yb_N	La_N/Yb_N	Y_N/Ho_N	Ce_N/Yb_N
01A/REE/STM	43.82	85.25	9.41	36.92	6.96	1.85	6.02	0.96	5.07	1.05	2.81	0.43	2.79	0.4	0.88	0.94	1.25	1.15	0.00	1.05
03/REE/STM	43.44	88.53	9.55	37.96	7.18	1.84	6.51	1.09	5.86	1.25	3.39	0.52	3.35	0.47	0.83	0.91	1.13	0.95	0.00	0.91
07/REE/STM	49.82	104.1	11.25	44.24	8.66	2.08	7.43	1.16	5.84	1.22	3.26	0.5	3.27	0.46	0.8	0.86	1.31	1.11	0.00	1.09
07A/REE/STM	36.13	66.07	7.89	30.06	5.83	1.27	5.03	0.83	4.21	0.9	2.49	0.38	2.47	0.36	0.72	0.92	1.18	1.07	0.00	0.92
14/REE/STM	65.25	176.60	15.04	60.30	13.20	3.25	12.60	2.13	11.76	2.43	6.53	1.02	6.26	0.91	0.77	0.74	1.16	0.76	1.21	0.97
15/REE/STM	48.71	97.57	10.42	40.25	7.41	1.86	6.34	1.02	5.31	1.13	3.03	0.48	3.15	0.44	0.83	0.98	1.17	1.13	1.13	1.06
17/REE/STM	43.11	80.10	9.06	34.19	6.36	1.52	5.64	0.91	4.92	1.05	2.85	0.45	2.87	0.41	0.78	1.02	1.14	1.11	1.10	0.96
18/REE/STM	43.19	84.62	9.53	36.11	6.80	1.70	5.86	0.98	5.25	1.12	3.09	0.49	3.20	0.47	0.83	0.95	1.06	0.99	1.11	0.91
33/REE/STM	31.79	59.17	6.32	23.99	4.09	0.79	3.58	0.84	3.34	0.64	2.13	0.33	2.19	0.34	0.63	1.16	0.94	1.06	1.36	0.92
34/REE/STM	36.09	67.12	7.57	29.82	5.35	1.06	4.77	1.11	4.30	0.80	2.48	0.38	2.46	0.36	0.65	1.01	1.12	1.07	1.28	0.94
35/REE/STM	35.53	66.70	7.46	29.21	5.17	1.01	4.52	1.04	4.08	0.76	2.38	0.36	2.34	0.35	0.64	1.03	1.11	1.10	1.38	0.97
36/REE/STM	40.34	74.04	8.47	32.90	5.81	1.19	4.96	1.19	4.60	0.86	2.78	0.43	2.84	0.43	0.68	1.04	1.01	1.04	1.14	0.90
08/REE/STM	23.35	45.85	4.982	19.73	3.67	0.901	3.11	0.53	2.716	0.589	1.631	0.256	1.593	0.217	0.82	0.95	1.14	1.08	1.24	1.00
09/REE/STM	36.46	71.87	7.978	30.61	5.542	1.241	4.849	0.769	4.102	0.882	2.424	0.397	2.489	0.366	0.74	0.99	1.13	1.08	1.12	0.99
10/REE/STM	35.74	68.38	7.589	28.62	5	1.026	4.175	0.688	3.639	0.763	2.093	0.329	2.143	0.307	0.69	1.07	1.13	1.23	1.14	1.10
11/REE/STM	14.96	29.67	3.306	12.43	2.268	0.589	1.908	0.307	1.658	0.336	0.944	0.152	0.945	0.139	0.87	1.00	1.17	1.16	1.40	1.07
11a/REE/STM	50.16	100.8	10.9	41.46	7.526	1.856	6.6	1.064	5.656	1.178	3.205	0.491	3.131	0.448	0.81	1.00	1.22	1.18	1.14	1.11
12/REE/STM	45.79	89.78	10.03	39.29	7.46	1.84	6.35	1.02	5.42	1.14	3.10	0.48	3.11	0.44	0.82	0.92	1.19	1.09	1.09	0.99
13/REE/STM	45.74	88.84	10.03	39.22	7.33	1.84	6.13	1.00	5.24	1.11	3.02	0.49	3.18	0.46	0.84	0.93	1.11	1.05	1.15	0.96
16/REE/STM	48.34	90.55	9.85	37.60	6.60	1.57	5.72	0.92	4.94	1.04	2.85	0.47	3.00	0.43	0.78	1.10	1.11	1.18	1.05	1.04
25a/REE/STM	36.99	68.75	7.84	30.76	5.60	1.04	5.00	1.18	4.61	0.85	2.61	0.39	2.52	0.37	0.6	0.99	1.15	1.08	1.29	0.94
26/REE/STM	34.25	63.25	7.24	28.58	5.26	0.99	4.62	1.11	4.31	0.80	2.52	0.38	2.40	0.36	0.62	0.97	1.11	1.05	1.32	0.91
29/REE/STM	31.48	58.63	6.67	26.05	4.77	0.88	4.14	0.96	3.69	0.67	2.04	0.30	1.95	0.29	0.61	0.99	1.23	1.18	1.26	1.03
30/REE/STM	42.68	87.33	9.36	36.57	6.92	1.49	6.14	1.46	5.76	1.07	3.28	0.50	3.22	0.48	0.7	0.92	1.11	0.97	1.16	0.93
30a/REE/STM	38.85	72.32	8.32	32.78	6.04	1.13	5.41	1.25	4.73	0.85	2.65	0.39	2.56	0.37	0.61	0.97	1.23	1.12	1.32	0.97
31/REE/STM	36.95	69.47	7.79	30.68	5.66	1.04	5.00	1.16	4.54	0.82	2.54	0.38	2.42	0.36	0.6	0.98	1.20	1.12	1.33	0.99
32/REE/STM	38.14	74.75	8.11	32.00	5.86	1.10	5.18	1.21	4.67	0.85	2.65	0.39	2.54	0.38	0.61	0.98	1.18	1.10	1.33	1.02
37/REE/STM	38.55	69.59	8.42	33.59	6.26	1.22	5.35	1.36	5.31	0.99	3.04	0.46	2.97	0.44	0.65	0.93	1.04	0.96	1.03	0.81
19/REE/STM	46.18	87.03	9.85	38.47	7.32	1.76	6.44	1.11	6.26	1.36	3.83	0.61	3.72	0.54	0.79	0.94	1.00	0.91	1.04	0.80
20/REE/STM	46.87	81.59	9.81	37.20	6.78	1.42	5.95	0.98	5.10	1.06	2.86	0.45	2.80	0.40	0.69	1.03	1.23	1.23	1.07	1.00
21/REE/STM	54.45	105.20	11.82	46.31	8.68	2.26	7.56	1.28	6.49	1.37	3.75	0.57	3.71	0.53	0.86	0.94	1.18	1.08	0.93	0.97
22/REE/STM	55.54	103.10	12.76	49.59	9.48	2.32	7.62	1.29	6.49	1.34	3.67	0.58	3.70	0.52	0.84	0.88	1.19	1.10	1.00	0.96
23/REE/STM	35.07	72.44	7.89	30.41	5.67	1.45	5.10	0.84	4.46	0.94	2.58	0.40	2.60	0.37	0.83	0.93	1.14	0.99	1.08	0.96
Normalizing values (Nakamura, 1974)	0.33	0.865	0.112	0.63	0.203	0.077	0.276	0.047	0.343	0.07	0.225	0.03	0.22	0.034	–	–	–	–	–	–

$Eu/Eu^* = (Eu)_{cn}/[(Sm)_{cn} \times (Gd)_{cn}]^{0.5}$

grains including both mineral and rock fragments were examined in representative 25 thin sections of sandstone with two thin sections for each sample for modal analysis. The petrographic samples were collected from thicker sandstone layers avoiding any other local lithological variations. The section measurement was carried out by precisely collecting field data on meter scale using tape-compass-clinometer method as per the procedure given in Compton (1962). The true thickness of the lithologies is calculated using the formulas proposed by Palmer (1916). The true thickness of individual lithotype viz. conglomerate, sandstone, siltstone, mudstone-shale was added separately and relative abundance was normalized to 100 that led to determine the ratio of conglomerate-sandstone–siltstone–mudstone in Lower, Middle and Upper Siwalik. The facies records were identified and marked in the stratigraphic column using Miall's classification (1996). The graphic artwork has been carried out on Corel-Draw software.

The major ion composition of the sediments provides significant information to assess the weathering intensity under prevailing climatic conditions that acted on the provenance. Thus, for both qualitative and quantitative characterization of weathering and paleoclimatic condition, Nesbitt and Young (1984) proposed the Chemical Index of Alteration (CIA) that evaluates the chemical weathering and transformation of various phases into secondary products (often clay/phyllosilicate) as compared to source rock. The quantitative CIA value is evaluated in terms of mol% of oxides using formula $CIA = [Al_2O_3/(Al_2O_3 + CaO^* + Na_2O + K_2O)^*100]$. The CaO* fraction represents the Ca content in the silicate-bearing minerals and its calculation is made on assumptions that if $CaO \leq Na_2O$, then CaO* value is taken as CaO value and if $CaO > Na_2O$, then Na_2O values are taken as CaO* value (Ali et al., 2021; Bock et al., 1998; Gallet et al., 1998; Roddaz et al., 2006).

5 Results

5.1 Field description

The sediments of Lower Siwalik are fine-grained, hard, compact with dominantly repeated flood plain sediments over channel sand (Fig. 3a) and frequent lateral shifting of the channel and few crevasse splay deposit. The presence of iron nodules in the rocks of Lower Siwalik is also noticed near Kalaunia (Fig. 3b). Mud pallets in the sandstone are signature of scouring of the active channel along its bank (Fig. 3c). The rocks of Lower Siwalik up-section grades into Middle Siwalik with a reduction in mud content and the sand-mud ratio is about 50–50 (Fig. 3d). The sandstone is thinly bedded to massive and medium-grained with some pebbly horizon. The thick sandstone layers form the multi-storeyed nature (Fig. 3e). The pebbles comprise quartzite, sandstone, mudstone indicating both intra-formational, as well as extra-basinal nature (Fig. 3f). The transition from the lower to the upper part of Middle Siwalik records the sudden decrease in mud content from 50% to almost 10–15% and increment in the rolling population of larger clasts (Fig. 3g). The clasts comprise quartzite, metabasic, slate, schist, granitic and gneissic fragments. The upper part of Middle Siwalik shows a higher degree of secondary calcification in the sandy layers in multi-storeyed sandstone forming calcretes and protruding out. These carbonate-cement bearing sandy layers are developed in subaerial vadose zone under warm and humid climatic conditions (Tandon & Varshney, 1991).

The size and frequency of the clasts increase in the upper part of Middle Siwalik. The sandstone is relatively loose and fragile. The size of clasts in the sandstone of Middle Siwalik reaches up to 10–15 cm. The further transition of Middle to Upper Siwalik is marked with a rapid increase in the size of clasts and thickness of conglomerate beds up to 30 m or even more. The conglomerate is matrix-supported (Fig. 4g) in the lower part but grades into clast supported up-section (Fig. 4h). The presence of sand lenses is an important feature of the conglomerate in the upper part (Fig. 3h). The larger clasts in conglomerate comprise quartzite, basalt, amphibolites, granite, gneiss, schist, phyllite and limestone. The upper part has medium- to coarse-grained, loose, friable sandstone with variegated mudstone in few horizons (Fig. 3g).

The measured section during field work in the Siwalik along Saj gad/Kalaunia gad—Sarra River indicates the development of various sedimentary facies (Fig. 4a–h). The section measurement results in the calculation of total true thickness of Siwalik about 3134 m. viz. Lower Siwalik (710 m), Middle Siwalik (2076 m) and Upper Siwalik (348 m) (Fig. 5a, b and c). The huge thickness of Middle Siwalik along Kalaunia gad is probably the second thickest sedimentation record in Uttarakhand Himalaya after Dun sub-basin (Ghosh & Kumar, 2000). The dominant lithofacies identified are massive silt and mud (Fsm), fine laminated silt and mud (Fl), massive and faintly laminated sand (Sm), horizontal laminated sand (Sh), ripple cross-laminated sand (Sr), planer cross-bedded sand (Sp), sand fine to coarse may be pebbly or group cross bedded (St), clast supported crudely bedded, horizontal bedding, imbrications (Gh) and matrix-supported massive gravel (Gmm) in various parts of the Siwalik Group (Fig. 5a–c). The lithofacies and their abbreviation are after Miall (1996).

5.2 Petrography

The sandstone petrography is a useful tool to address the source area lithology and provenance studies. Petrographic

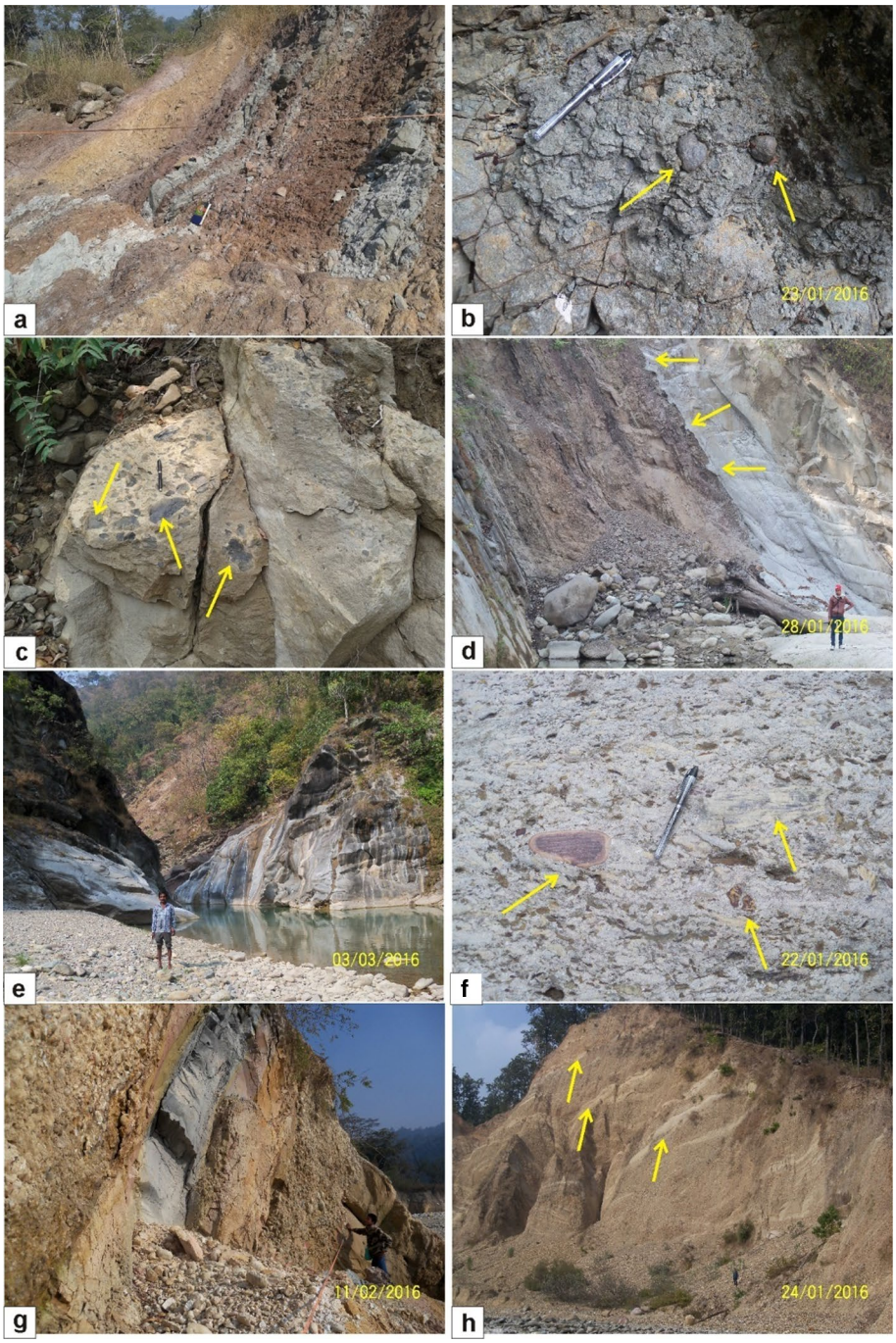

Fig. 3 Field photographs of Siwalik rocks showing **a** Variegated mudstone in Lower Siwalik **b** Development of iron nodules in mudstone of Lower Siwalik **c** Mud pallets in the sandstone **d** Thick mudstone–sandstone association in Middle Siwalik. Note the development of load cast structure at the contact **e** Multistoried sandstone in Middle Siwalik **f** Quartzite and shale lithic fragments in Lower Siwalik sandstone **g** Mudstone sandwiched between conglomerate beds in Upper Siwalik **h** Sandstone lenses in the conglomerate in Upper Siwalik

study of the Siwalik sandstone was carried out of the representative 25 unaltered coarse- to fine-grained, sandstone and mudstone samples from different horizons of the Lower to Upper Siwalik Subgroup. During the petrographic study, the varieties of quartz and other detrital constituents were described following the methods given by Krynine (1940) and Folk (1980). The monocrytalline and polycrystalline quartz grains were separately noticed and their relative abundance was taken into consideration along with feldspar (potash and plagioclase, separately), mica and other lithic fragments (Basu et al., 1975; Dickinson, 1985; Ingersoll & Suczek, 1979).

5.2.1 Lower Siwalik

Quartz (70 to 90%) is the dominant constituent grain in the rock. Monocrystalline quartz (Qm) has a high abundance over polycrystalline quartz (Qp) (Fig. 6A). The rock

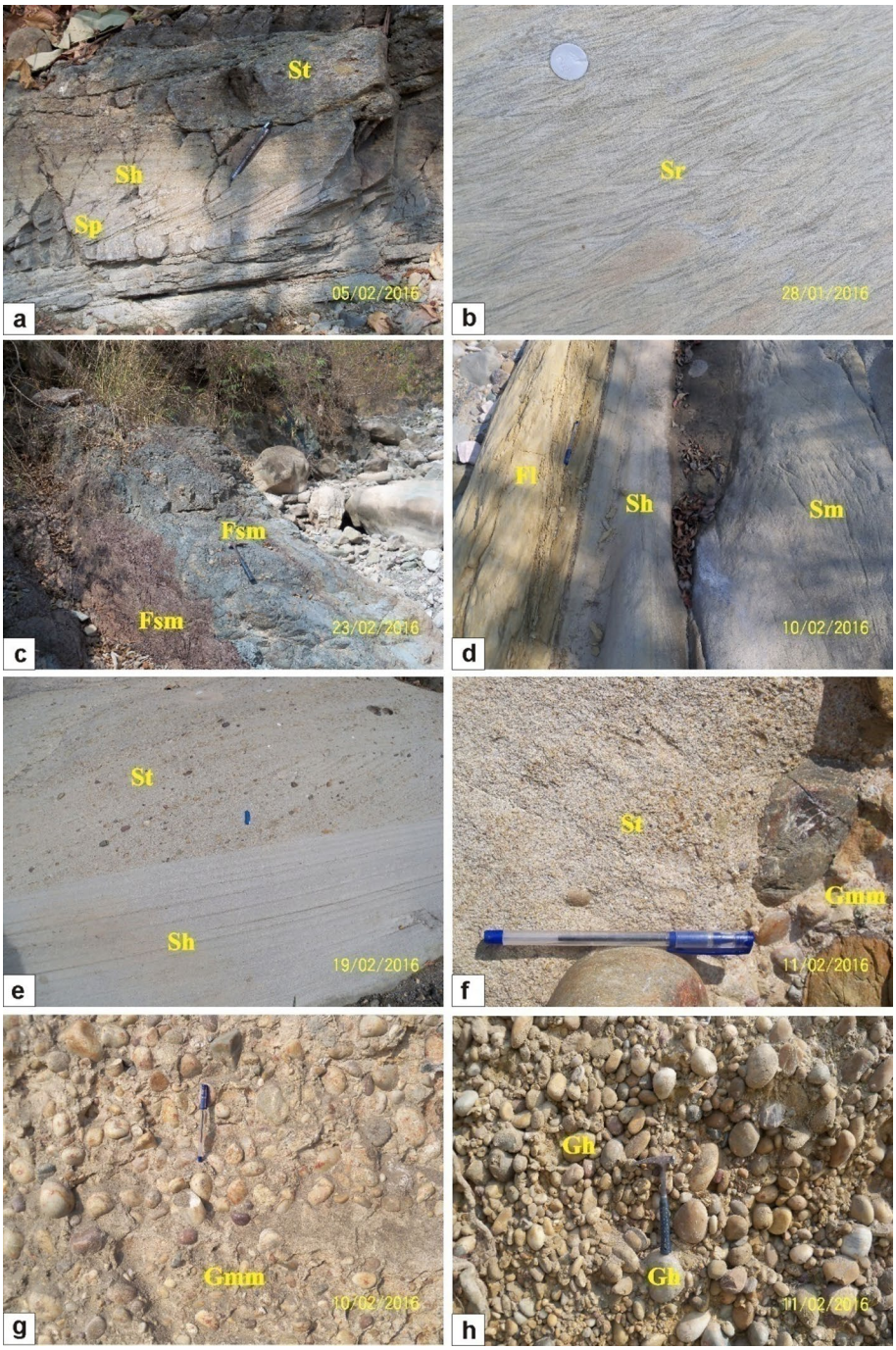

Fig. 4 Field photographs showing **a**–**h** development of various sedimentary facies in Lower to Upper Siwalik rocks. Facies classification after Miall (1996), Abbv: massive silt and mud (Fsm), fine laminated silt and mud (Fl), massive and faintly laminated sand (Sm), horizontal laminated sand (Sh), ripple cross laminated sand (Sr), planer cross bedded sand (Sp), sand fine to coarse may be pebbly or group cross bedded (St), clast supported crudely bedded, horizontal bedding, imbrications (Gh) and matrix supported massive gravel (Gmm)

contains 5 to 20% mica (biotite dominating) with very few grains of feldspar (1 to 5%) qualifying this sandstone into the quartz-arenite as dominant lithology whereas a few samples straddle between sublitharenite to the sub-arkosic field (Folk, 1974) (Fig. 9). Both the feldspar; K-feldspar and plagioclase, are present and former is in relatively higher proportion. The twining in the detrital feldspar of Lower Siwalik sandstone is common feature. Mica flakes are aligned and the tight packing of quartz grains is due to high compaction and/or overburden related lithostatic pressure. However, sandstone of the Lower Siwalik has a siliceous matrix, sometimes calcareous and ferruginous cement, up to 5% in the interstitial space of clasts/detrital grains. The sandstone of the Lower Siwalik is mineralogically and texturally matured, very fine to fine-grained, well-sorted and tight to moderately packed. Maturity, fine grain, high roundness, high compactness and less weathering of the constituting grains of the rock represent long transportation and prolonged burial. The fine mudstone

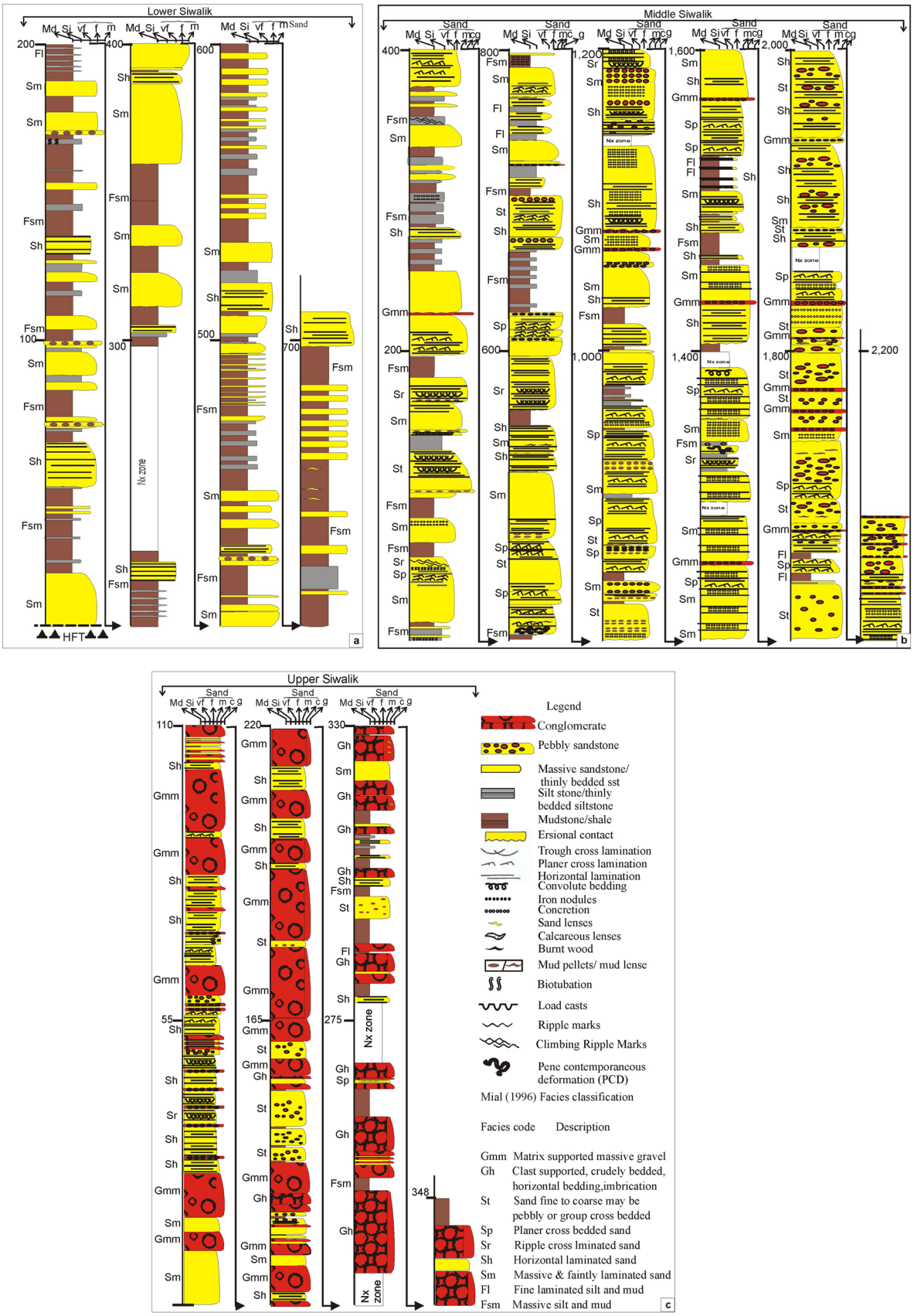
Lower Siwalik
Middle Siwalik
Upper Siwalik
Nx zone
HFT
a
b
c
Legend
Conglomerate
Pebbly sandstone
Massive sandstone/ thinly bedded sst
Silt stone/thinly bedded siltstone
Mudstone/shale
Ersional contact
Trough cross lamination
Planer cross lamination
Horizontal lamination
Convolute bedding
Iron nodules
Concretion
Sand lenses
Calcareous lenses
Burnt wood
Mud pellets/ mud lense
Biotubation
Load casts
Ripple marks
Climbing Ripple Marks
Pene contemporaneous deformation (PCD)
Mial (1996) Facies classification
Facies code Description
Gmm Matrix supported massive gravel
Gh Clast supported, crudely bedded, horizontal bedding,imbrication
St Sand fine to coarse may be pebbly or group cross bedded
Sp Planer cross bedded sand
Sr Ripple cross lminated sand
Sh Horizontal laminated sand
Sm Massive & faintly laminated sand
Fl Fine laminated silt and mud
Fsm Massive silt and mud

◂**Fig. 5** Litho-log of the Siwalik succession in Saj Gad–Sarra River section showing various sedimentary facies with measured thickness for each sub-group: **a** Lower Siwalik; **b** Middle Siwalik; **c** Upper Siwalik

samples show very small quartz grains associated with clay and silt. The lithic fragments of shale are also noticed in the mudstone (Fig. 6b).

5.2.2 Middle Siwalik

In the lower part of Middle Siwalik, sandstone shows dominancy of quartz over feldspar and lithic fragments. The grains are sub-angular to sub-rounded, moderately sorted and well packed in the lower part of the Middle Siwalik but in younging direction, grains are texturally immature and comprise angular to sub-angular, loosely packed and poorly sorted in the upper part of the Middle Siwalik. Grains show sutured and concave-convex contact, probably due to the reaction of carbonate cement with quartz and lithic fragments (Ghosh & Kumar, 2000). The lower part of Middle Siwalik sandstone comprises quartz grains (~ 70%); both monocrystalline quartz (~ 85%) and polycrystalline quartz (~ 15%), mica; both muscovite and biotite, (~ 20%), feldspar; both plagioclase and potash, (5 to 10%) and lithic fragment (~ 10–12%) (Fig. 6c and d). The proportion of feldspars and the lithic fragment is increased in the upper part of Middle Siwalik (Fig. 6e and f). Compositionally, the sandstone (< 15% matrix) falls in the sublith-arenite field with a little quartz-arenite composition. A few samples with > 15% matrix are classified under arkosic-greywacke composition (Fig. 7). The sandstone shows a higher proportion of lithic fragments and feldspar than Lower Siwalik, hence, mineralogically and texturally it is relatively less-matured. Plagioclase shows albite twinning whereas the cross-hatched twining is noticed in the microcline. The feldspar sometimes shows weathered nature. Presence of kinked mica, fractured quartz grains, Qp, undulose extinction in quartz show deformed metamorphic source rock. Qp is formed by the development of sub- grains within the large quartz grain under the process of sub-grain rotation in dynamic recrystallization (Passchier & Trouw, 1995). Lithic fragments are metamorphic (quartzite, schist, phyllite) and sedimentary rocks (shale, sandstone). Sandstone comprises calcareous (calcite) and ferruginous (iron oxide) cement, and siliceous matrix (quartz) binding the framework grains. Well-developed calcite can be appreciated in thin sections as a result of secondary precipitation (Fig. 6c). The gradual increment in the proportion of calcareous cement and decline in ferruginous cement and siliceous matrix from Lower to Middle Siwalik is noticed.

5.2.3 Upper Siwalik

The Upper Siwalik sandstone is medium to coarse-grained, angular to sub-angular, immature, poorly sorted and moderate to loosely packed. The constituting grains are quartz (30–50%), feldspars (10–20%), lithic fragments (10 to 50%) and mica (5–10%) (Fig. 6g–j). Matrix/cement is siliceous, ferruginous and calcareous (10 to 30%). The sandstone is classified as lithic greywacke to feldspathic greywacke composition (Folk, 1974) (Fig. 7). Calcite as cement shows high order interference color, and siliceous matrix shows dark grey to grey appearance. The grains are sometimes surrounded by reddish-brown to opaque ferruginous cement which is in high proportion to other binding materials. Quartz grains are Qp or composite quartz (numbers of crystals with different orientations within a grain boundary) as well as Qm (Fig. 6g and h). Lithic fragments and feldspar grains are in high abundance in the Pinjor Formation of the Upper Siwalik. Lithic fragments include platy fragments of shale, schist and mylonite gneiss, granite gneiss, and large fragments of sandstone and quartzite (Fig. 6i and j). The platy nature of shale, schist, mylonite and gneissic rock fragments is a result of derivation from a cleaved or foliated source rock containing abundant platy minerals. Distinguishable large sandstone fragments and schist having mica rich flakes showing preferred orientation are common features. Along with these, large detrital of polycrystalline quartz, and shale represent metamorphic and sedimentary source rock, respectively. Sub-grain development within large quartz grain is the result of sub-grain boundary rotation under the dynamic recrystallization process in the metamorphic rock and depicts the derivation of the grain from the deformed metamorphic source rock. Lithic fragments of shale are common in the sandstone of the Pinjor Formation. Mylonite gneiss fragment can be appreciated with the presence of alternate thin component bands of stretched or ribbon quartz grains and feldspar and darker mica flakes; biotite, in the sandstone. Grains of twinned plagioclase crystals at the right angle, kinked muscovite flakes, fresh microcline and K-feldspar are present in the sandstone. Twinned crystals of plagioclase feldspar represent igneous protolith. The igneous source rock for the sediments is evidenced by the presence of microcline and perthite texture in K-feldspar. Kinked mica is the product of deformation and hence originated from the deformed source rock. Large size, high angularity and less to un-weathered nature of rock fragments and grains give clues about less transportation of the constituents. The heavy mineral constituents of the sandstone comprise medium to high grade metamorphic minerals like garnet, kyanite along with some accessory phases like zircon, apatite, rutile and tourmaline. These are principally derived from acidic rocks like granite and granite

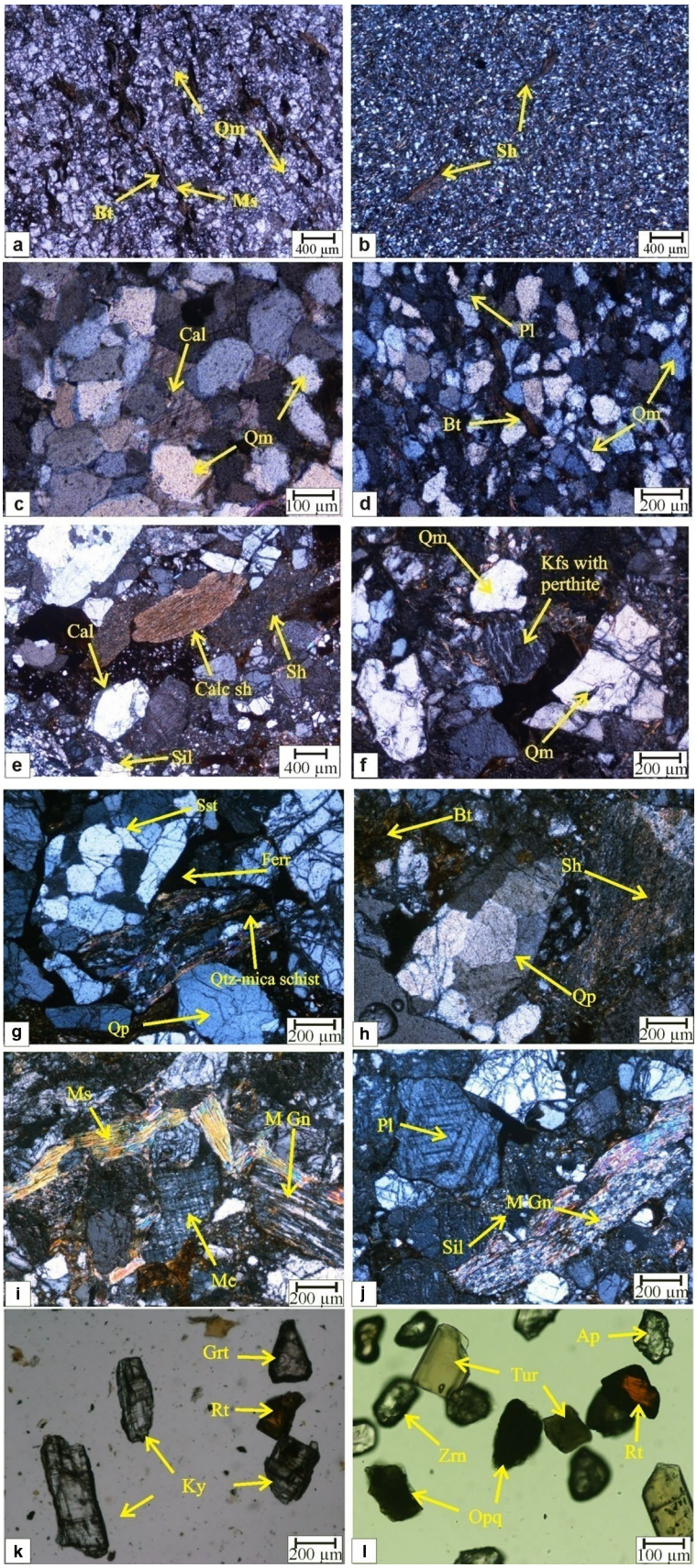

Fig. 6 Photomicrograph of the samples showing: **a** Fine grained sandstone of Lower Siwalik, showing mus-bt and Qm; **b** Lithic fragments of shale with fine grained quartz in mudstone of Lower Siwalik; **c** Medium grained sandstone with rounded to sub-rounded quartz and calcite grown in intergranular spaces; **d** Medium grained sandstone showing pl-bio-Qm assemblage. **e** Lithic fragments of shale, calc-shale with siliceous and calcitic matrix; **f** K-feldspar with perthite texture and large monocrystalline quartz indicating granitic source area; **g** Lithic fragment of quatz-mica schist and sandstone indicating mixed provenance of sedimentary and metamorphic terrain; **h** Polycrystalline quartz with biotite and shale association; **i** Microcline feldspar with mylonitic gneiss and muscovite as detrital composition; **j** Presence of pl and mylonitic gneiss. Both **i** and **j** support the derivation of sediments from igneous, as well as high grade metamorphic terrain in the provenance. **k** and **l** Presence of heavy minerals like grt-ky-rt-tur-ap-zrn-opq derived from acidic igneous and high-grade metamorphic rocks. Abbr: Qm; quartz monocrystalline, Qp: polycrystalline quartz, pl: plagioclase, bt: biotite, mus: muscovite, grt: garnet, ky: kyanite, rt: rutile, tur: tourmaline, ap: apatite, zrn- zircon, opq: opaque (mineral abbreviations after Whitney & Evans, 2010)

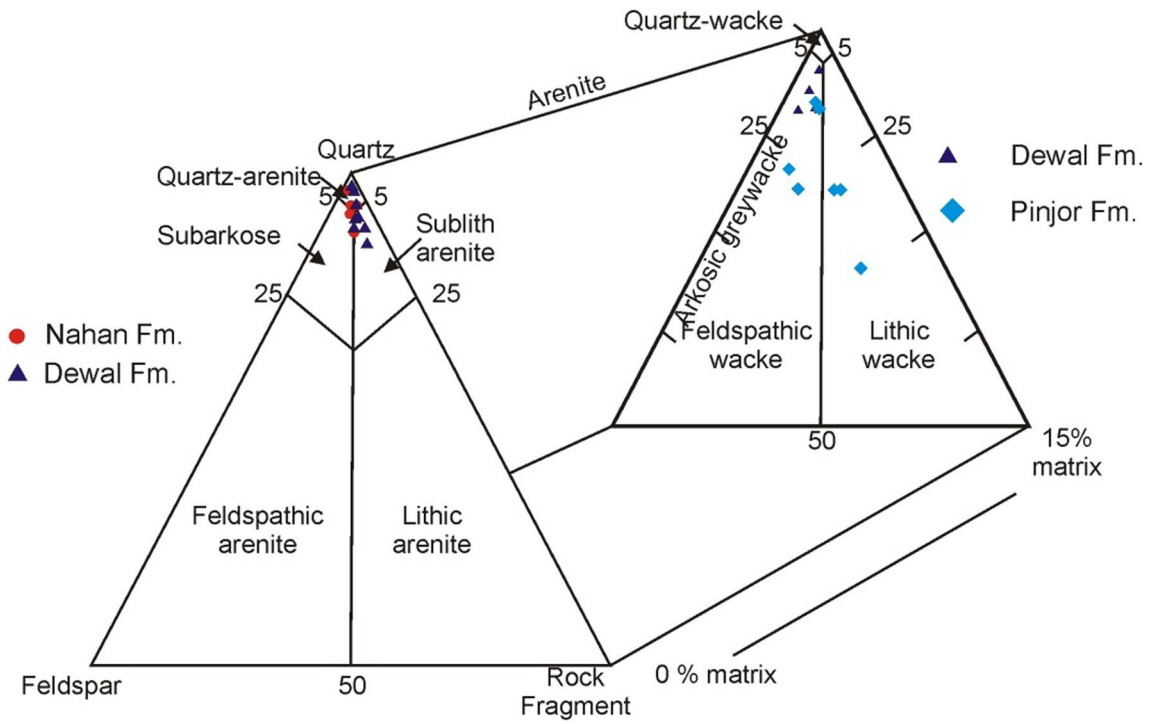

Fig. 7 Sandstone classification schemes of the Pettijhon et al. (1973) showing composition of the sandstone in Siwalik Group

gneiss (Fig. 6k and l). The high-grade metamorphic minerals and accessory phases start appearing from Middle Siwalik sandstone up-section as Lower Siwalik sandstone dominantly contains iron oxide and magnetite—hematite association.

5.3 Grain size

The lower part of Middle Siwalik sandstone has grain size ranging from very fine to medium-grained, occasionally coarse (mean graphical grain size 1.18 to 1.21Φ) in nature. The upper part behaves similarly with a slight increase mean graphical grain size (1.16 to 1.31Φ). The sediment sorting is better in the upper part. The Upper Siwalik sandstone shows mean graphic grain values of about 1.08–1.51 Φ. The skewness values range between − 0.042 to − 0.071 in Middle Siwalik and − 0.095 to + 0.159 in Upper Siwalik. The kurtosis values of the grain size variation range from 0.598–0.683 in Middle Siwalik whereas 0.604–1.112 in Upper Siwalik, suggesting platykurtic to platykurtic–Mesokurtic nature, respectively.

5.4 Geochemistry

5.4.1 Major oxide

The geochemical composition of mudstone in the Siwalik shows variation at various stratigraphic levels (Table 1). The major element composition confirms the abundance of SiO_2 ranges from 57.01 to 86.24 wt%, while Al_2O_3 ranges from 4.84 to 19.37 wt%. Harker Variation Diagram are prepared for total silica and alumina variation in mudstone against all other oxide values (Fig. 8) indicating a fairly correlation of silica with Na_2O and MgO. This correlation suggests the presence of sodic-plagioclase and involvement of mafic constituents like olivine, pyroxene and biotite in the source region, as well as their altered products like illite, chlorite and smectite. However, the Na_2O content is always < 1 in the studied samples and a higher K_2O/Na_2O ratio suggests the dominance of potash feldspar over sodic plagioclase. Whereas Al_2O_3 ($r = -0.89$), K_2O ($r = -0.84$), FeO^t ($r = -0.86$) and TiO_2 ($r = -0.51$) (to some extent) display strong linear negative arrays with silica point towards the reduction in kaolinite content and presence of other Fe-Ti bearing phases like ilmenite, up-section. The SiO_2/Al_2O_3 ratio increases from Lower (4.18 avg.) to Middle Siwalik (6.64 avg.) indicating a progressive increase in quartz content (Ranjan & Banerjee, 2009) and variable contents of aluminous clay and quartz in the samples. Further in Upper Siwalik (4.16 avg.), the ratio decreases due to increase in variation in lithic fragments indicating mixed provenance. The scattering of the other oxides as CaO and P_2O_5 against silica is noticed. The variation diagrams exhibit positive correlation of K_2O ($r = 0.92$), TiO_2 ($r = 0.74$), and FeO^t ($r = 0.84$) whereas Al_2O_3 displays negative linear plots with Na_2O ($r = -0.57$) and slightly with MgO ($r = -0.47$)

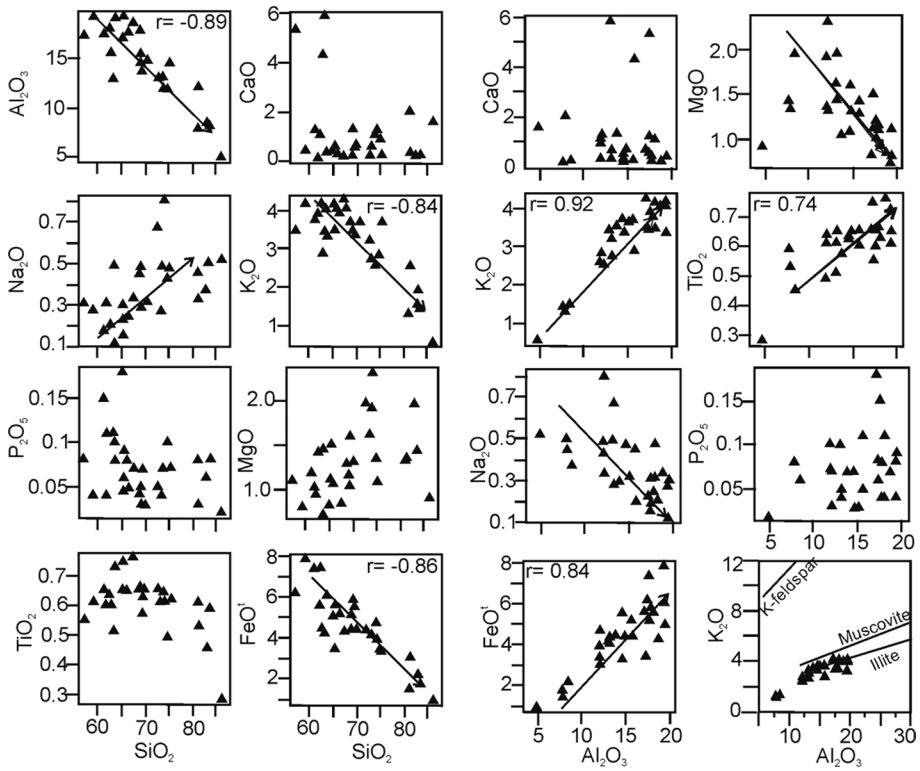

Fig. 8 Harker Variation Diagram of the mudstone of Siwalik Group of all oxides against silica and alumina

(Fig. 8). Like silica, CaO and P_2O_5 remain scattered against the alumina too. The positive correlation between alumina and potash indicates the presence of potash feldspar and clay mineral control, i.e., illite in the mudstone composition. The variation diagram also indicates all the data plots near the muscovite-illite line (Fig. 8) suggesting alteration of potash-feldspar and muscovite, derived from felsic rocks like granite and granite gneiss. Such alteration takes place under moderate to intense weathering in humid climatic conditions. The Post Archean Australian Shale (PAAS) normalized major oxide values (after Taylor & McLennan, 1985) opine about the enrichment of silica and depletion of rest of the major oxides with strong negative Na_2O and MnO anomalies. The Cao and K_2O exhibit wide variation (Fig. 11a).

Hayashi et al. (1997) suggested Al_2O_3/TiO_2 ratio varies between 21 and 70 for felsic rocks within the silica range of 66–76%. The positive correlation of Al_2O_3 with TiO_2 and FeO^t, Al_2O_3/TiO_2 ratio (13.15–31.61) and total silica content (57.01 to 86.24 wt%) in the mudstone suggest the association of Ti- bearing phases with clay fraction and abundant Fe-Ti bearing independent phases like biotite, chlorite, ilmenite, titano-magnetite and opaques, derived principally from basic suits and their low-grade metamorphic products along with the felsic component. The presence of biotite and ilmenite in heavy minerals and chlorite in clay minerals further support the geochemical interpretation.

The binary classification schemes have been proposed to classify the chemistry of sediments in various litho-fields (Herron, 1988; Pettijohn et al., 1973). In the binary plot of Pettijohn et al. (1973) between log (SiO_2/Al_2O_3) vs log (Fe_2O_3/K_2O), the present mudstone chemistry straddles between shale and wacke with a few samples in the lithic-arenite field (Fig. 9a) whereas the mudstone samples show greywacke to lithic-arenite composition in the log (SiO_2/Al_2O_3) vs log (Na_2O/K_2O) classification schemes of Herron (1988) (Fig. 9b). The Lower and Middle Siwalik sandstone are classified as quartz arenite, sublitharenite to the sub-arkosic field and where the matrix is > 15% as in upper Middle and Upper Siwalik, are classified as arkosic-greywacke to lithic greywacke and feldspathic greywacke.

5.4.2 Trace element geochemistry

Trace Element concentrations of the studied Siwalik sediments are given in Table 2. Concentrations of the Large Ion Lithophile Elements (LILE) like Ba, Sr and Rb range between 383 and 1155 mg kg^{-1} (avg. 727); 18–96 mg kg^{-1} (avg. 52.75) and 36–191 mg kg^{-1} (avg. 142), respectively. Their vide variation is noticed in the studied samples due to their high mobility during weathering, diagenesis and low-grade metamorphism (Wronkiewicz & Condie, 1987). Barium is enriched whereas Sr is highly depleted against the PAAS and Upper Continental Crust (UCC) (Nance & Taylor, 1976; Taylor & McLennan, 1985). Rubidium shows a strong positive correlation with the alumina ($r = 0.84$) and K ($r = 0.94$) whereas scattering nature is displayed by Ba

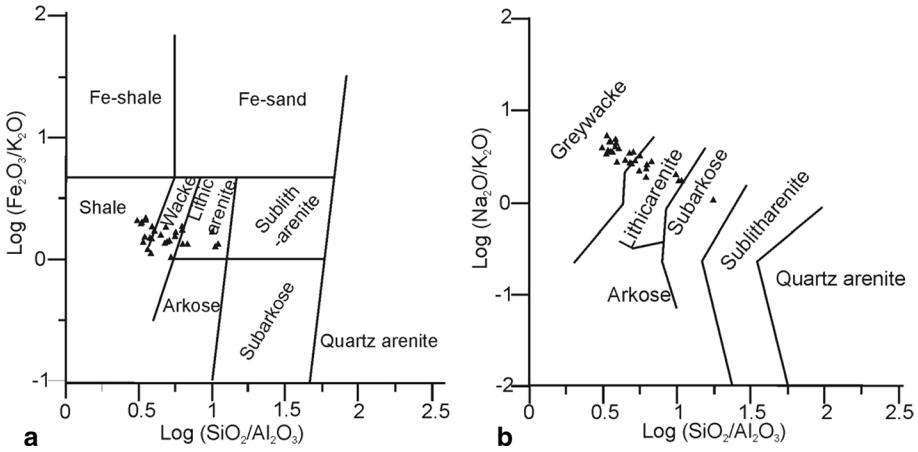

Fig. 9 Geochemical classification of the mudstone in Siwalik Group on: **a** Herron (1988)'s log (SiO_2/Al_2O_3 vs log (Fe_2O_3/K_2O) binary plot and; **b** Pettijohn et al (1973)'s log (SiO_2/Al_2O_3 vs log(Na_2O/K_2O)

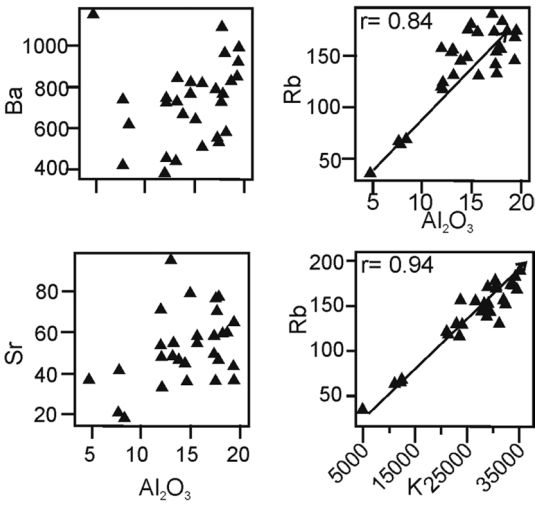

Fig. 10 Bivariate plots of LILE (Large Ion Lithophile Elements) against alumina and potassium showing chemical variation in the mudstone samples

and Sr content (Fig. 10). The HFSE prefers the felsic rock over the mafic one and these elements range between 13 and 81 mg kg^{-1} (Y), 126 and 357 mg kg^{-1} (Zr) and 5 and 20 mg kg^{-1} (Nb). Yttrium and Zr show enrichment against the PAAS and UCC values (Table 2). Niobium is often noticed as a negative anomaly (Fig. 11c) and is depleted in the granite and granite gneiss from Higher and Lesser Himalayan Crystallines of Kumaun Himalaya (Islam et al., 2005; Rao & Sharma, 2009, 2011). The average values of transition elements like Cr, Sc, V, Co, Ni are 73, 16.44, 103, 75.13 and 30.03 mg kg^{-1}, respectively. It suggests the enrichment of Sc and Co and depletion of Cr, V, and Ni against the PAAS. The minor depletion of Cr and Ni suggests less contribution from the mafic rocks in the source. Th and U contents vary between 12 and 20 and 1.81 and 5.95 mg kg^{-1}, respectively. The binary plots of alumina against the transition elements (Fig. 12) indicate a strong positive correlation of alumina with V, Ni ($r = 0.86$ for both) and Cr ($r = 0.74$).

5.4.3 Rare earth element geochemistry

Results of REE from the present study are given in Table 3. The ΣREE ranges between 69.61 and 377.27 mg kg^{-1}, which is most of the time higher than UCC (146.37 mg kg^{-1}) and occasionally higher than PAAS (184.86 mg kg^{-1}). Although there is no significant variation noticed in the REE content towards younging direction in the measured section yet a few samples from the upper Middle and Upper Siwalik shows relatively higher REE contents (> 200 ΣREE). This may be attributed to the exhumation of basement gneisses and granites in the Higher Himalaya and crystalline klippen during the deposition of Middle-Upper Siwalik sediments. The PAAS normalized REE plot points towards the relative enrichment of LREE and depletion of HREE with prominent positive Eu anomaly (Fig. 11b). The normalized values of the REE closely resemble the Upper Continental Crust values (Taylor & McLennan, 1985). The chondrite–normalized REE plots shown in Fig. 11d indicate a more or less uniform pattern with slopping LREE and near-flat HREE content. The LREE/HREE ratio is high (11.15–15.11) with a significant negative Eu anomaly ($Eu/Eu^* = 0.6–0.88$). The ratio of the important REE suggests the depletion in La_N/Sm_N (0.74–1.16), Gd_N/Yb_N (1.01–1.31; one sample 0.94), La_N/Yb_N (0.76–1.23), Y_N/Ho_N (0.93–1.4), and Ce_N/Yb_N (0.8–1.11) contents.

5.5 Paleo-alteration indices

The calculated values of CIA from the present investigation vary from: 55.8 to 78.7 for Lower Siwalik; 53 to 78.3 for Middle Siwalik, with one sample showing 49.9 and; 58.8 to 81.7 for Upper Siwalik sediments. This is an indication of moderate weathering when these data are compared with the 'Average Shale' value of 70–75 (Visser & Young, 1990). The unweathered igneous rocks have CIA values of about 50 (Nesbitt and Young, 1984) and most of the samples exceed

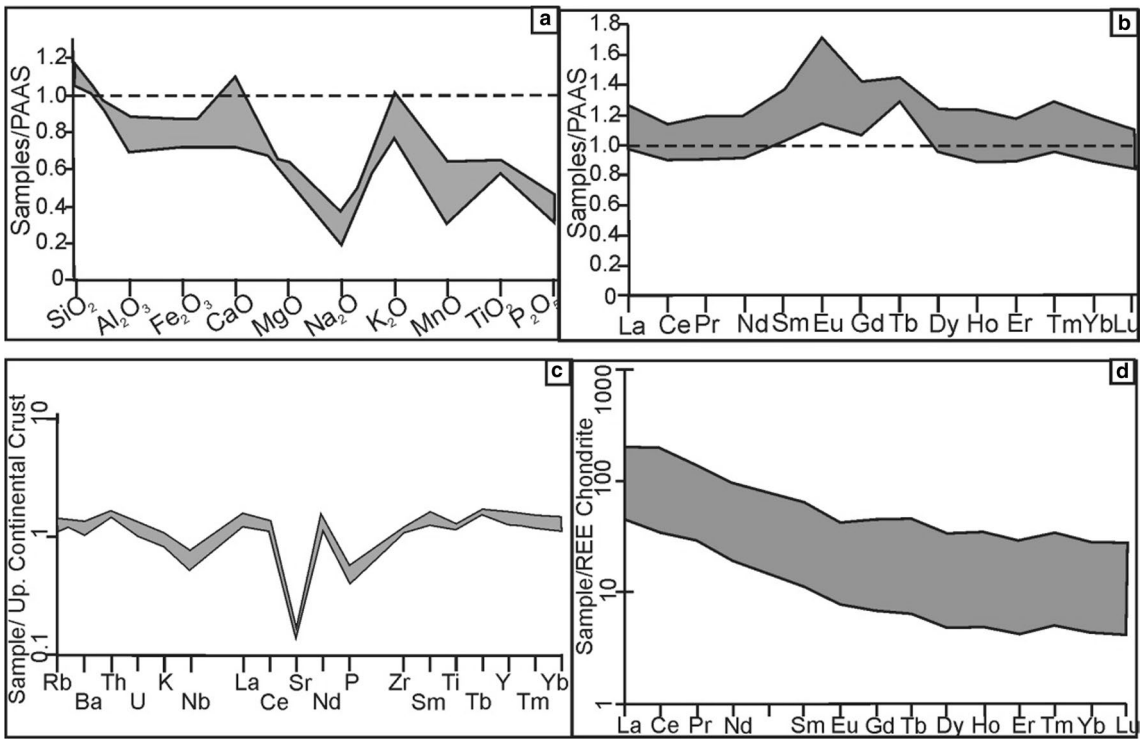

Fig. 11 PAAS normalized **a** Major oxide and **b** Rare Earth Element (REE) distribution in mudstone samples. **c** Upper Continental Crust (UCC) normalized Trace element distribution pattern in the mudstone samples, **d** Chondrite normalized REE pattern of the mudstone samples in Siwalik Group. PAAS values after Taylor and McLennan (1985), UCC values after Taylor and McLennan (1989)

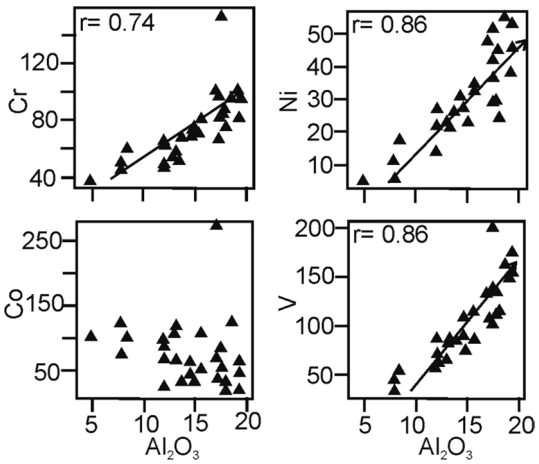

Fig. 12 Bivariate plot of the transition elements against alumina showing strong positive correlation of Cr, Ni, and V with alumina

this value. A few samples although show higher values between 75 and 81.7 and indicate intensely weathered provenance. The Plagioclase Index of Alteration (PIA) values {PIA = $Al_2O_3/(Al_2O_3 + CaO + Na_2O)*100$} in most of the samples surpass 60, which is a threshold value for moderate to low weathering conditions (Fedo et al., 1995, 1996) further confirming the intensely weathered provenance.

The relative proportions of alkali, alumina and calcium oxide (Al_2O_3–$CaO^* + Na_2O$–K_2O) in molecular proportion can be used to address the source rock composition in the A-CN-K ternary classification scheme (Nesbitt & Young, 1984). The unaltered igneous rocks occupy the place near A-CN join with CIA values near 50. Any level of weathering in these primary rocks will plot away towards the A-K join related with enrichment of alumina and potash. The most altered rocks host the clay minerals like kaolinite, gibbsite, chlorite, illite, muscovite, etc. The data clustering in the A-CN-K ternary plot lies towards the illite field indicating a large contribution from clay minerals and depletion of Na-Ca related to the decomposition of plagioclase (Fig. 13a).

6 Discussion

6.1 Source characteristic (provenance)

Petrographically, the Siwalik sandstone is classified as quartz arenite with subordinate sublitharenite and sub-arkose in present study area (Pettijohn et al., 1973). The same is confirmed on the Ternary classification scheme of Q–F–L indicating quartz arenite to sublitharenite, subfeldsarenite

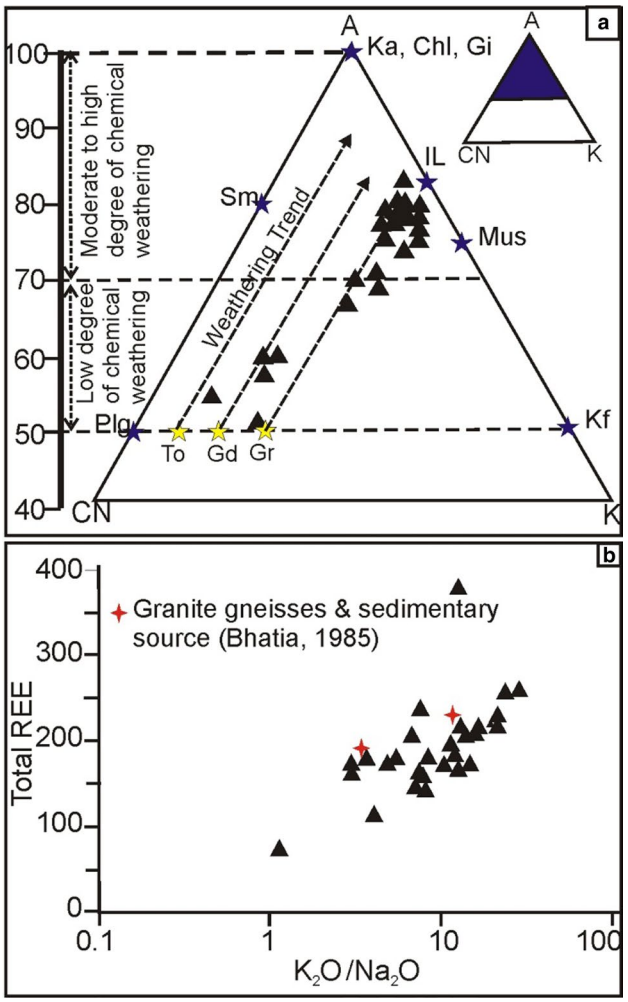

Fig. 13 **a** Ternary A-CN-K plot of the mudstone (after Nesbitt & Young, 1984) of the mudstone samples; A-Al_2O_3; C-N-Cao + Na_2O; K-K_2O (mol prop.); Abbv: Sm-smectite, Ka-Kaolinite, Chl-chlorite, Gi-gibbsite, Mus-muscovite, Il-illite, Kf-k-felspar, Plg-plagioclase. Data for To (Tonalite), Gd (granodiorite) and Gr (granite) is from Condie (1993). The arrows indicate the weathering trends of these rocks. **b** Bivariate plot of alkali ratio vs total REE after Bhatia, 1985. The red stars indicate the locations of granite gneiss and sedimentary sources

and a few represents the lithic feldsarenite to feldspathic litharenite (Folk, 1974) (Fig. 16a). It indicates low relief of the source area with stable tectonic conditions. In stratigraphic direction, the sandstone becomes more sublitharenite with matrix > 15% in a few samples. Stratigraphically, the younger part has received a higher proportion of feldspar and rock fragments indicating their lithic and feldspathic greywacke composition. The presence of the twinned and perthitic nature of feldspar indicate their igneous protolith. Mono and polycrystalline quartz, bent mica and the lithic fragment of mica schist, gneisses indicate the derivation of sediments from a deformed and metamorphic terrain. The polycrystalline quartz grains indicate the effect of cataclastic deformation in the source area. This is further evidenced with the presence of high grade metamorphic and heavy minerals like garnet, kyanite, biotite, tourmaline and opaques, sourced from highly metamorphosed provenance. The zircon, ilmenite, apatite and titanite are scattered in the thin sections from various stratigraphic levels being representative of granitoids and other felsic igneous rocks in the source region. These rocks are abundantly present in the Kumaun Himalayan region. The grain size of sandstone in Middle Siwalik indicates saltation and suspension processes as a major mode of transportation and dominant over traction or rolling population. The saltation population has a steep curve indicating well-sorted grain but the curve flattens in suspension load due to poorly sorted sediment. High variation in traction load content is noticed in the Upper Siwalik sandstone indicating streams with changing energy condition.

The chemistry of fine-grained clastic sedimentary rocks has been demonstrated to investigate the provenance and tectonic setting, as well as variation in sedimentary processes such as weathering conditions, climatic factors, and post-depositional changes (Cox et al., 1995; Cullers, 1994; McLennan et al., 1993). The identification and characterization of the provenance based on the geochemical signatures of sediments have been carried out (Floyd and Leveridge 1987; Cullers 1994; Armstrong-Altrin et al., 2004). Both mobile and immobile elements and their ratios are categorized as useful input to decipher the provenance studies to a diverse extent. The presence of immobile elements such as REE and HFSE carry constructive information to determine the composition of the source rock as these elements remain unaffected during weathering and transportation (Bhatia & Crook, 1986). The Siwalik sedimentation records have been brought out with geochemical and detrital geochronological input in many sections of the Himalaya (Ali et al., 2021; Mandal et al., 2018; Najman, 1995, 2006; Najman & Garzanti, 2000; Ranjan & Banerjee, 2009; Sinha et al., 2007) but the spatial variations in the litho-packages along the strike in the Himalaya viz. presence or absence of eclogites, various klippe and nappe units, differential exhumation records with varying metamorphic assemblages, geochronology of lithounits and along-strike variation in the thrusting events are contributory factors for exposing the varieties of lithologies in the temporal frame. Thus, the nature and composition of Siwalik sedimentation is resulted from a combination of many such factors and justifies its along-strike variation within the foreland basin.

The PAAS normalized major oxide values indicate the enrichment of silica suggesting the upper crustal material as a major source of the sediments. The depletion in the Na_2O and wide variation in the CaO suggests moderate to strong weathering conditions and their removal during weathering and transportation. The major oxide and their

ratio are widely used to describe the provenance signatures and tectonic setting of deposition. Roser and Korsch (1986) utilized the bivariate plot of SiO_2 and K_2O/Na_2O ratio to discriminate the principle tectonic setting of deposition viz. Passive Margin, Active Continental Margin, Oceanic Island Arc setting. The bivariant plot of the SiO_2 and K_2O/Na_2O of the mudstone of the Siwalik Group in the Nandhaur Sanctuary area shows the clustering of the samples in the Passive Margin field (Fig. 14a). The Passive Margin tectonic setting of the provenance is further confirmed on the K_2O/Na_2O vs SiO_2/Al_2O_3 plot (Maynard et al., 1982) (Fig. 14b). The Siwalik sediments have been characterized as molasse deposit. These sediments are deposited in the foreland basin that was developed in the frontal part of

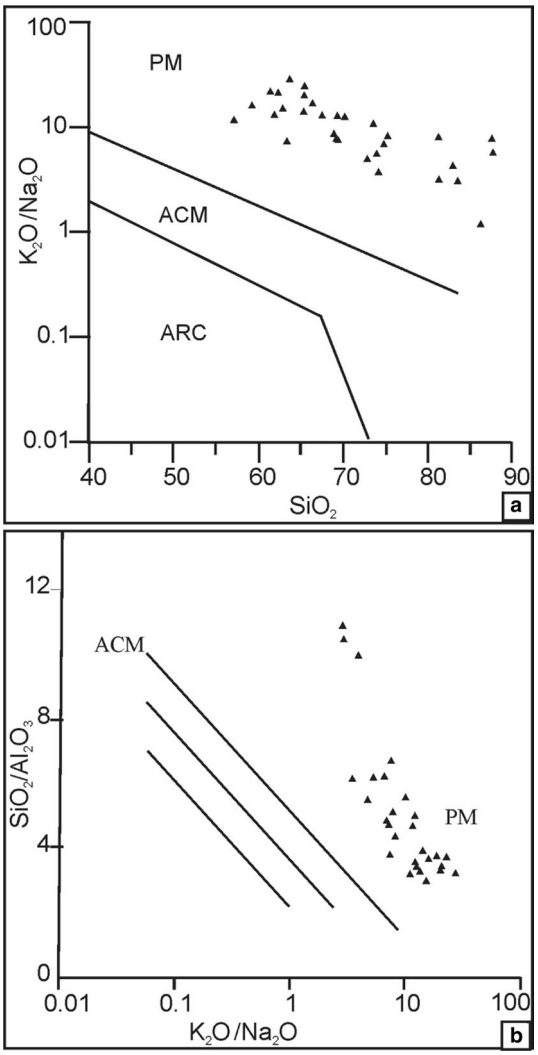

Fig. 14 Tectonic discrimination bivariate plot of the Siwalik sediments. **a** After Roser and Korsch (1986) **b** After Maynard et al. (1982). Both the binary plots show Passive Margin field of sediments deposition. Abbv: PM: Passive Margin; ACM: Active Continental Margin; ARC: Continental Arc

India-Eurasian collision. However, the chemistry of Siwalik sediments represents the Passive Margin tectonic setting which is actually inherited provenance signature, preserved in the finer clastic sediments of Siwalik. The reduction in the average ratio of K_2O/Na_2O from Lower to Middle Siwalik also suggests the change in the provenance from the low-grade metasedimentary association to high-grade metamorphic rocks. The Al_2O_3/TiO_2 appears very promising in the determination of the nature of the source rock (Andersson et al., 2004; Garcia et al., 1994; Hayashi et al., 1997) as the immobile nature of Al and Ti during weathering qualifies them to use their ratio as strong provenance signatures. Willis et al. (1988) proposed the range of Al_2O_3/TiO_2 between 3 and 8 for mafic igneous rocks, 8 and 21 for intermediate and 21 and 70 for felsic rocks, whereas later a broader range was provided as < 14 for mafic rocks and 19–28 for felsic rocks as provenance (Hayashi et al., 1997). The Al is hosted in the feldspar whereas Ti is retained in the mafic minerals like pyroxene, amphiboles, biotite and some accessory phases like ilmenite and rutile. Hence the values of the ratio increase with evolved magma and their products. The Al_2O_3/TiO_2 ratio in the Siwalik sediments in the present investigation varies between 13.15 and 31.61 indicating a mixed/variety of rocks in the provenance with intermediate to felsic being dominated. The REEs are considered as immobile elements and their total abundance and ratio are not disturbed during weathering and metamorphism. Bhatia (1985) correlated the sum of REE and alkali ratio in the sediments and proposed the fields for granite-gneiss and sedimentary sources. The Siwalik mudstone from study area plots near these granite gneiss and sedimentary sources (Fig. 13b) in K_2O/Na_2O vs ΣREE plot (Bhatia, 1985). Cox et al. (1995) proposed the Index of Compositional Variability (ICV) to measure the degree of chemical weathering. The ICV is dependent on the relative abundance of alumina over other oxides but silica and is indication of behavior of clay minerals against the non-clay silicate minerals. The value of ICV indicates the maturity of the mudrocks. Potter et al. (2005) proposed the relation of ICV against the CIA to relate the sediments to its provenance. This binary plot illustrates the weathering trends of three principle crustal magmatic rocks; granite-andesite-basalt (Fig. 17b). The Siwalik mudstone shows the affinity of its sediments dominantly with granite-andesite though minor but important contribution from basaltic rocks (Fig. 1717b). The Himalaya has a variety of Proterozoic–Palaeozoic granitoids in various tectonic belts such as in Central Crystallines, Almora-Ramgarh, Chiplakot, Askot klippe rocks and intrusive granites viz. Amritpur, Dudhatoli, Champawat, and Cenozoic leucogranites (Debon et al., 1986; Islam et al., 2005; LeFort, 1988; Sharma et al., 2011) along with sedimentary rocks of low or almost no metamorphism, especially in the Outer Lesser Himalaya. All these units have thus contributed the sediments to the

foreland basin. The precise characterization of the source area lithologies can be made on the classification scheme of Herron (1988) based on SiO_2/Al_2O_3-Na_2O/K_2O plot. The mudstone chemistry from present study plots in greywacke to lithic arenite field with one sample in subarkose field. In the classification scheme of Pettijohn et al. (1973), the chemical composition of the mudstone shows affinity with shale-wacke and extends up to the lithic arenite field.

The clastic sedimentary rocks preserve the trace element ratio as in their parental rocks and are widely used in provenance study, primary source composition, the extent of heavy mineral content and sediment recycling. The wide variation of LILE is noticed in the studied samples related to their high mobility during weathering, diagenesis and low-grade metamorphism (Wronkiewicz & Condie, 1987). The positive correlation of LILE against alumina is indicative of strong control of phyllosilicate minerals over their distribution (Sinha et al., 2007). Although Rb content varies in the Siwalik sediments yet its positive correlation with K is due to the presence of illite as one of the major clay minerals, as illite prefers large ionic radii cations like Rb, K, Cs over smaller ones (Na, Ca and Sr) during weathering (Nesbitt et al., 1980; Wronkiewicz & Condie, 1987). The scattering values of Ba and Sr also indicate that they are derived from granitic rocks in the Himalaya, which are depleted in these elements (Islam et al., 2005), and the smaller size of Sr over Ba qualifies it to be leached out of the weathering profile, whereas Ba is absorbed in clay minerals. Also, the depletion of Sr is strongly indicative of plagioclase dominated intensely weathered source terrain, especially under sub-aerial weathering conditions. Thus, the scattering of these elements is indicative of clay dominated as well as plagioclase bearing granitoids and basic rocks.

The least mobile elements, such as HFSE, REE, Th, Sc, Hf and Co, which remain unaffected during weathering, transportation, post-depositional changes and metamorphism (Taylor & McLennan, 1985) are taken into consideration to evaluate the source rock lithologies. Th and Zr show incompatible behavior and are enriched in felsic rocks whereas Sc is a compatible element that has affinity with mafic rocks. The recycling processes do not affect the Th/Sc ratio (McLennan et al., 1993). The binary plot between Th/Sc and Zr/Sc, proposed by McLennan et al. (1993) has Th/Sc on the vertical axis being a good indicator of magmatic differentiation processes and Zr/Sc on the horizontal axis which represents the measure of mineral sorting and recycling (Taylor & McLennan, 1985). The Th/Sc and Zr/Sc ratios range from 0.75–2.00 to 5.90–30.88 in the studied mudstone, respectively. These values are indicative of felsic rock as a source in comparison to mafic rocks. Further on the Sc vs Th/Sc plot, the mudstone samples are clustered near Rampur Group (≡Rautgara), Chakrata pelites and Chandpur Formation and in the vicinity of Chakrata quartzite and Nagthat Formation indicating these are a few of the provenance (Fig. 17a). The mudstone samples plot in a cluster mostly in the Upper Continental Crust and near the PAAS

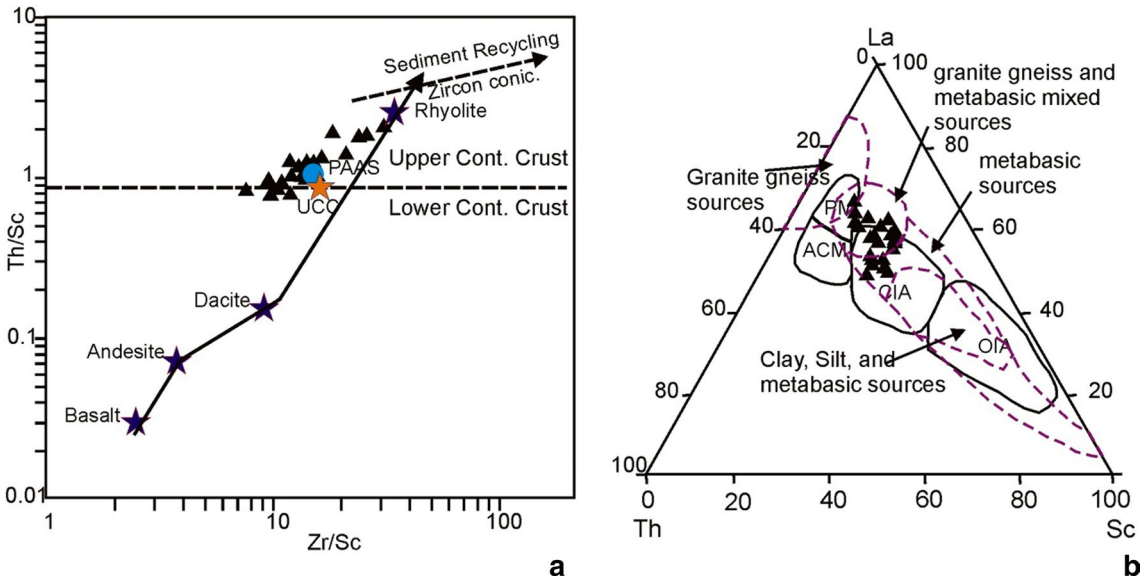

Fig. 15 **a** Trace Element Th/Sc vs Zr/Sc diagram of Mudstone samples from Siwalik (after McLennan et al., 1993). Average volcanic rocks plotted after Roser and Korsch (1999). Solid line represents the compositional trend, dashed line represents sediment recycling and zircon saturation. The PAAS and UCC compositions are also plotted for comparison. All the samples show affinity with UCC field. **b** La-Th-Sc Ternary Discrimination Plot showing source composition and tectonic setting of sediment deposition. The darker line fields are after Bhatia and Crook (1986); dotted line fields are after Cullers (1994). Abbv: PM: Passive Margin; ACM: Active Continental Margin; CIA: Continental Arc; OIA: Oceanic Island Arc

(Fig. 15a). Their trend is almost parallel to the evolutionary trend of volcanic suits from basalt to rhyolite (Roser & Korsch, 1999). The UCC normalized trace element contents in the mudstone show strong Sr, P, Nb and Ti anomalies. The negative Sr, Nb and Ti anomalies are often associated with syn-collisional granites. The negative Ti and Sr are associated with fractional crystallization of biotite and plagioclase fractionation, respectively. The Paleo-Meso Proterozoic granites of the Himalaya display the negative anomalies of Sr, Ti, Nb and P (Chauhan, 2015; Das et al., 2019; Islam et al., 2005; Rao & Sharma, 2011) suggesting that these granites and their gneissic variants along with metasedimentaries are also important sources of the sediments. The other significant ratios of the immobile trace elements are La/Sc, Cr/Th, Th/Co, and La/Co which are reliably used for assessment of provenance composition of sedimentary rocks (Armstrong-Altrin et al., 2004; Cullers, 2000). The range for these ratios in the studied mudstone sample is La/Sc (0.71–5.86), Cr/Th (2.42–9.50), Th/Co (0.07–0.95), and La/Co (0.15–2.31) which mostly lies within the range of sediments derived from the felsic sources. However, Th/Co values straddle between the felsic and mafic sources and indicate the mixed source rocks. The various trace element ratios are given in Table 4 for a comparison with felsic and mafic provenance along with PAAS and UCC values.

The transition elements like Cr and Ni are severely associated in the mafic and ultramafic suits and sulfide minerals, although in trace amount, play a significant contribution in tracing the provenance lithologies. The crustal abundance of Cr and Ni are 100 and 75 mg kg^{-1} (Taylor, 1964), respectively, whereas in basaltic magma these elements are concentrated up to 200 and 150 mg kg^{-1} (Nockolds & Allen, 1956; Turekian, 1963; Vinogradov, 1962). Their depletion is noticed in the felsic magma thus low concentration of these elements into sediments are indicative of their protolith being felsic in nature. The Cr and Ni concentration in sediments > 150 mg kg^{-1} and > 100 mg kg^{-1}, respectively, and their low ratio between 1.3 and 1.5 and bearing high correlation coefficient ($r = 0.9$) altogether opine their derivation from mafic/ultramafic suite. The present study reveals the low Cr; 37–152 mg kg^{-1} (avg.73) and Ni 5–55 mg kg^{-1} (avg. 30.03) contents in Siwalik mudstone. The higher Cr/Ni ratio (1.7–7.67) and their fairly good correlation with each other ($r = 0.75$) suggest a little derivation of the sediments from the mafic/ultramafic suit.

The REEs are considered as highly immobile in nature and carry information related to magmatic evolution, differentiation and signature of melting material during magma generation. The LREE and HREE content, along with a significant normalized elemental ratio of Eu/Eu*, La_N/Sm_N, Gd_N/Yb_N, La_N/Yb_N, Y_N/Ho_N and Ce_N/Yb_N contribute notably to understand the magmatic processes. The relative occurrence of LREE and HREE vary in mafic to felsic rocks with mafic being generally richer in HREE and thus has a low LREE/HREE ratio. On the contrary, the high LREE/HREE ratio and negative Eu anomaly are characteristic of felsic rocks (Cullers, 1994). As the REE remains inert during weathering, alteration and metamorphism, they carry key signatures in interpreting the provenance of sediments (Taylor & McLennan, 1985). In the studied mudstone samples, the ΣREE ranges between 69.61 and 377.27 mg kg^{-1} and higher than UCC most of the time (146.37 mg kg^{-1}) and occasionally higher than PAAS (184.86 mg kg^{-1}). In the ΣREE vs K_2O/Na_2O binary plot, the data are scattered near the granite gneiss and sedimentary sources (Bhatia, 1985) indicating these rocks as the primary source for the sediments. The chondrite normalized REE pattern shows sloping LREE and near-flat HREE contents where LREE/HREE ratio is high (11.15–15.11) with significant negative Eu anomaly (Eu/Eu* = 0.6–0.88) and are strongly indicative of their derivation from fractionated and evolved felsic source. Though few samples show no anomaly and indicate the presence of basic rock in the protolith that has supplied the calcic plagioclase retaining Eu in their lattice. The rocks of Higher Himalaya have granite gneiss and granite as major lithologies including basic intrusive along with the presence of basic extrusive–intrusive rocks and felsic intrusive in Lesser Himalaya together have contributed significantly during the Siwalik sedimentation. The sediments of Lesser and partly Higher Himalaya were deposited in passive margin setting in the northern age of Indian plate (Acharyya, 1990; Ahmad et al., 2000; Brookfield, 1993). The paleocurrent directions obtained from the Lesser and Higher Himalaya indicate transport direction of sediments towards NNW-NNE (Ganesan, 1975; Myrow et al., 2003; Valdiya, 1970) suggesting the sediments were derived from south such as Aravalli Supergroup, Delhi Supergroup, Bundelkhand granitoids, etc. In Siwalik Group the paleocurrent analysis reveals transport direction in channels towards south indicating the origin/provenance of the Siwalik sediments in north, the Himalaya (Ghosh et al., 2003; Kumar et al., 1999). The PAAS normalized REE patterns show variable REE content in the mudstone sample with almost similar trends that also point out the evolved crustal material. The Gd_N/Yb_N ratio varies between 1.01 and 1.31 with one sample showing 0.94 value. This range matches well with the sediments derived from Post-Archean upper crustal rocks, in absence of any hydrodynamic sorting of heavy phases during transportation (McLennan et al., 1993) which is also corroborated by scattering of Zr against Gd_N/Yb_N in the studied samples (Supplementary Material 1). The chondrite normalized Himalayan granitoids in Kumaon Himalaya viz. in Higher Himalayan Crystallines, in Chiplakot, Askot, Almora klippe and nappe units, Bhilangana, Debguru and Amritpur granitoids also show high LREE/HREE ratio, strong negative Eu anomaly and sloping LREE and flat HREE content (Chauhan et al.,

2013; Das et al., 2019; Mehta, 1993; Rao & Sharma, 2011). Thus, the chondrite and PAAS normalized REE content of the studied mudstone samples indicate their derivation from the evolved crustal material like granite and granite gneisses both from Higher Himalaya, their equivalent thrust sheets and Lesser Himalayan region along with a contribution from metasedimentary rocks as well.

6.2 Paleo-weathering conditions

In the A-CN-K ternary plot of Nesbitt and Young (1984) the samples origin around granite-granodiorite source near A-CN join and trends depart towards the A-K join indicating moderate to high chemical weathering (Fig. 13a). The maximum number of samples lies near the illite-muscovite field on A-K join above 70 CIA values supporting the removal of Na–Ca by leaching and enrichment of K_2O during weathering and conversion of feldspar into clay minerals (Nesbitt et al., 1980) indicating severely weathered provenance. The K_2O values in the mudstone are up to 4.24%, eroding the possibility of potash metasomatism to enrich the K_2O content. The samples remain scattered along with the trend, especially near the illite field and are characteristic of provenance under non-steady state weathering, resulted from the Cenozoic tectonics and rapid exhumation of the rocks during thrusting in Himalaya that further promote the rapid erosion of the soil and rocks. Thus, clay minerals have significant control on mudstone chemistry. The ICV values for the Siwalik mudstone in the present investigation vary between 0.59 and 1.18, suggesting that mudstone is chemically matured (Cox et al., 1995). A few less weathered samples indicate their derivation from a highly unstabilized source rock, probably rapidly exhuming Himalayan lithounits along various thrusts that hampers the weathering processes. Although the age of MCT has been proposed between 23 and 17 Ma (DeCelles et al., 2001; Thakur, 1992) with some younger ages around 9–7 Ma (Macfarlane et al., 1992), yet the erosion and upliftment of Higher Himalayan Crystallines and emplacement of crystalline nappes were operated between 11 and 7.50 Ma, the post Lower—Middle Siwalik boundary viz. 11 Ma (Ghosh & Kumar, 2000; Valdiya, 1999), though the development of Lesser Himalayan Duplex system initiated about 12.5 Ma, still very close to the above-said age (DeCelles et al., 2001). Hence the Higher Himalaya has not started eroding its sediments to a substantial level before 11 Ma and the Lesser Himalaya was also not being rapidly exhumed as MBT remained active between 11 and 5 Ma thus Higher and Lesser Himalayan sequence was under relatively steady-state and supplied the highly weathered sediments along with some relatively less weathered products to the foreland basin. Thus, provenance before 11.0 Ma, mudstone of Lower Siwalik received sediments from, was under relatively steady-state and supported the stability and allowed the intense weathering processes. This is further supported by the strongest weathering condition reported in the Himalaya during Middle Miocene time, probably related to the extra influence of higher temperature during the climatic optimum (Clift et al., 2008; Zachos et al., 2001). The Middle Siwalik sediments aged 11.0–5.3 Ma. (DeCelles et al., 1998; Ghosh & Kumar, 2000; Sinha et al., 2005), exhibit extreme variations in the degree of weathering point out the non-steady state conditions in the provenance. The unstable provenance in Himalayan region was result of rapid exhumations along the major thrusts like MCT, Ramgarh Thrust (RT), nappe boundaries and specially MBT that was active during the same time frame. Thus, there remained little time for the effective weathering processes to act upon and sediments were eroded from partially to incomplete weathered profiles and regoliths. After the 5.3 Ma, although many of the thrusts were ceased yet the MBT, various back-thrusting structures and intra-formational thrusts within Siwalik were active/reactive and thus supplied the sediments from the various intensity of weathered levels during the deposition of Upper Siwalik (Catlos et al., 2001; Chauhan et al., 2022; DeCelles et al., 2001; Harrison et al., 1997; Huyghe et al., 2001). The presence of quartzite clasts in high frequency (dominantly of Nagthat and Ramgarh quartzite) in the Upper Siwalik conglomerate supports the proximity of the provenance to the foreland basin.

6.3 Tectonic setting

The petrographic modal analysis (after Basu et al. 1975; Mack and Suttner 1977) indicates the composition of sandstone as quartzarenite to subfeldsarenite-sublitharenite with minor as lithic-feldsarenite to feldspathic litharenite (Folk, 1974). The Siwalik sediments represent the "Recycled Orogen" tectonic setting in the Q–F–L ternary classification (Fig. 16b). Two important criteria are used SiO_2 vs K_2O/Na_2O plot (after Roser & Korsch, 1986) and log (K_2O/Na_2O) vs log (SiO_2/Al_2O_3) (after Maynard et al., 1982) to classify the nature of tectonic setting during sedimentation viz. Passive Margin (PM), Active Continental Margin (ACM) and Continental Arc (ARC). The mudstone samples from the present study are plotted in the PM Field in both the binary plots indicating that the sediments were deposited in a Passive Margin tectonic setting. The same is further confirmed on the ternary plot of La-Th-Sc proposed by Bhatia and Crook (1986) and Cullers (1994) where the samples straddle between the Passive Margin and Continental Island Arc setting (Fig. 15b). However, the Siwalik rocks are well-known Molasse sediments, deposited in dynamic fluvial setting in the Foreland Basin developed in front of the rising Himalaya thus the Passive Margin tectonic setting is the provenance geochemical signatures that are inherited from the source of the sediments. The Proterozoic to Early Paleozoic sediments

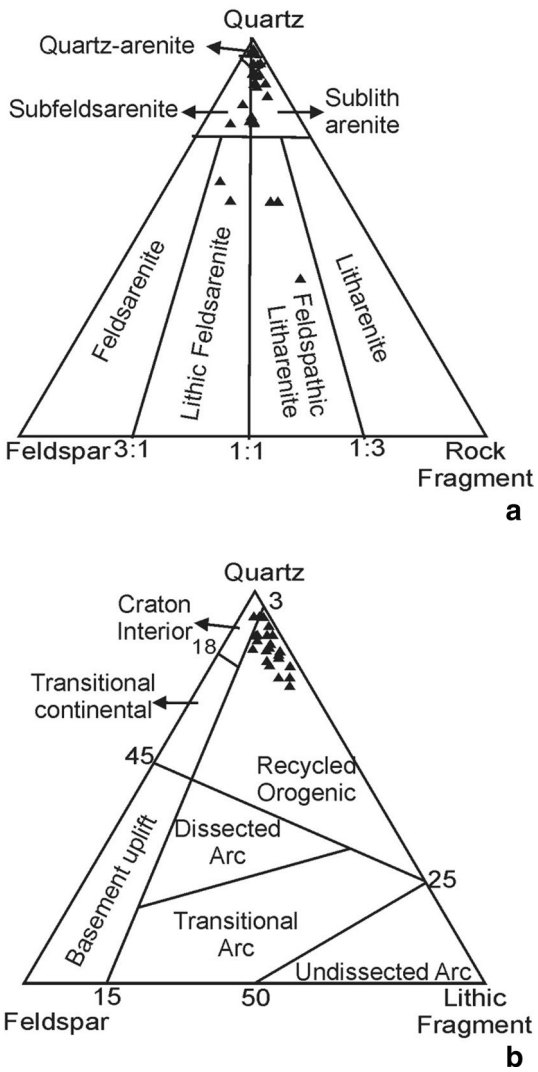

Fig. 16 **a** Q-F-Rf (quartz-feldspar-rock fragments) ternary diagram showing composition of the sandstone based on relative detrital modes (after Folk, 1974) **b** Q–F–L (quartz-feldspar-lithic fragment) ternary diagram indicating various provenance (Dickinson, 1985)

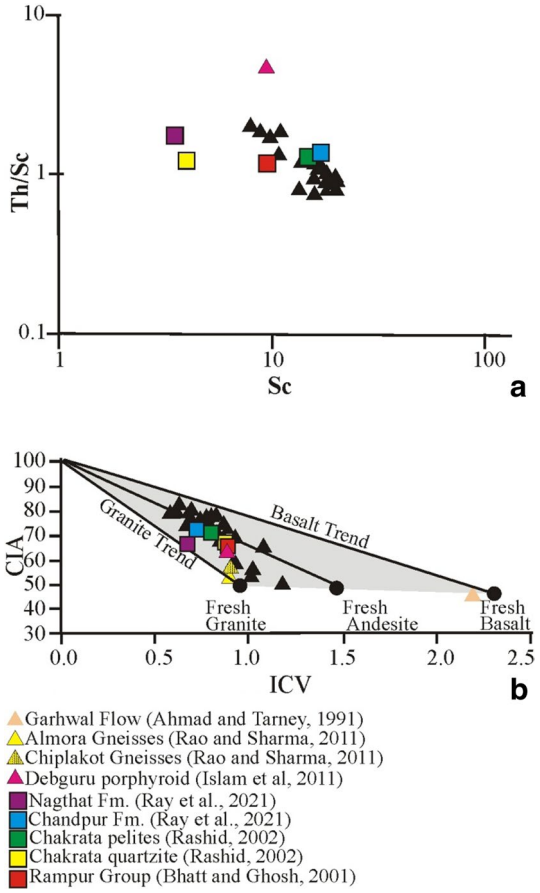

Fig. 17 **a** Sc vs Th/Sc binary plot of mudstone **b** Binary plot of ICV vs CIA values (after Potter et al., 2005) indicating sediments supplied from mixed felsic-mafic sources. The published data of various sources from Himalaya are also shown for comparison (symbols for both the diagrams are same)

of Lesser Himalaya are believed to be deposited on Passive Margin of Indian plate (Brookfield, 1993; Frank et al., 1977) whereas the granite and granite gneiss of Higher Himalaya and their equivalent nappe/klippe bears the signature of syn-collisional to Paleo Proterozoic Island Arc Setting (Kohn et al., 2010; Rao & Sharma, 2011) being the source rocks for the sediments.

7 Conclusions

The chemical signatures in mudstone of the Siwalik Group are studied to address these sediments to their protolith units. The Th/Sc vs Sc values links these mudstones with various tectono-stratigraphic units in Lesser and Higher Himalaya as prominent suppliers of sediments. The REE values also points towards the origin of sediments from evolved felsic crustal source rocks with minor contribution from mafic suits.

The geochemical distribution in mudstone is governed by the dominance of clay minerals like illite and kaolinite. The mudstone is derived from the weathering of the mixed source rock of felsic, mafic and metasedimentary rocks in the provenance that were deposited in the Passive Margin tectonic setting. This is also confirmed on the Th/Sc vs Zr/Sc ratios.

The Siwalik mudstone with their weathering trends and high CIA values, indicate the moderate to highly weathered provenance subject to different climatic conditions. Various parameters of weathering in Siwalik mudstone geochemically match with the present day exposed lithounits of Lesser and Higher Himalaya further confirms their derivation from Himalayan region.

Table 4 Trace and REE ratio from mudstone samples from Nandhaur Sanctuary area, the similar ratios from felsic and mafic sources, PAAS and UCC using various references are also shown for comparison

Elemental ratio	Siwalik (present Study)	Felsic rock-derived sediment range[a]	Mafic rock-derived sediments range[b]	Post Archeasn Australian Shale (PAAS) values[c]	Upper Continental Crust values[d]
La/Sc	0.71–5.86	2.50–16.3	0.43–0.86	3.40	2.21
Th/Sc	0.75–2.0	0.84–20.5	0.05–0.22	1.18	0.79
Cr/Th	2.42–9.50	4.0–15.0	25–500	4.61	7.76
Th/Co	0.07–0.95	0.67–19.4	0.04–1.40	0.15	0.63
La/Co	0.15–2.31	1.80–13.8	0.14–0.38	0.67	1.76
Eu/Eu*	0.6–0.88	0.40–0.94	0.71–0.95	0.64	0.63

[a]Cullers, (1988, 1994, 2000); Cullers et al (1988); Cullers and Graf (1984)

[b]McLennan (2001); Taylor and McLennan (1985)

[c]Nance and Taylor (1976)

[d]Chondrite normalized

The signature of weathering intensity varies from Lower to Upper Siwalik sediments and indicate steady to non-steady state provenance during the foreland basin deposition. This is also related with the development of Himalayan thrust kinematics that played a significant role in providing the variety of clasts to the Himalayan Foreland Basin during Middle Miocene to Lower Pleistocene age.

Supplementary Information The online version contains supplementary material available at https://doi.org/10.1007/s43217-022-00106-6.

Acknowledgements The present work is part of the approved Field Season Program of Geological Survey of India Northern Region during F.S. 2015-16 and has been funded under item code: STM/NR/UK/2015/002. The HOD, GSI NR and Dy. D.G., SU: UK are thanked to provide the necessary facility to carry out this work. Publication Division, GSI NR is thankfully acknowledged for arranging the review and permission to communicate this manuscript. The authors convey their sincere thanks to the Chemical Division and Petrology Division, GSI NR for providing chemical analysis and petrographic slides, respectively.

Data availability All the datasets generated during the course of this study and are related to this work have been included in this manuscript.

Declarations

Conflict of interest There is no direct–indirect financial or non-financial competing interest related with the present manuscript with any person or organization.

References

Acharyya, S. K. (1990). Pan-Indian Gondwana plate break-up and evolution of the northern and eastern collision margins of the Indian Plate. *Journal of Himalayan Geology., 1*, 75–91.

Ahmad, T., Harris, N., Bickle, M., Chapman, H., Bunbury, J., & Prince, C. (2000). Isotopic constraints on the structural relationships between the Lesser Himalayan Series and the High Himalayan Crystalline Series, Garwhal Himalaya. *Geological Society of America Bulletin, 112*, 467–477. https://doi.org/10.1130/0016-7606(2000)112%3C467:ICOTSR%3E2.0.CO;2

Ali, S., Phartiyal, B., Taloor, A., Arif, M., & Singh, B. P. (2021). Provenance, weathering, and paleoclimatic records of the Pliocene-Pleistocene sequences of the Himalayan foreland basin, NW Himalaya. *Arabian Journal of Geosciences, 14*, 198. https://doi.org/10.1007/s12517-021-06461-4

Andersson, P. O. D., Worden, R. H., Hodgson, D. M., & Flint, S. (2004). Provenance evolution and chemostratigraphy of a Palaeozoic submarine fan-complex: Tanqua Karoo Basin, South Africa. *Marine and Petroleum Geology, 21*, 555–577.

André, L., Deutsch, S., & Hertogen, J. (1986). Trace-element and Nd isotopes in shales as indexes of provenance and crustal growth: The early Paleozoic from the Brabant Massif (Belgium). *Chemical Geology, 57*(1–2), 101–115. https://doi.org/10.1016/0009-2541(86)90096-3

Armstrong-Altrin, J. S., Lee, Y. I., Verma, S. P., & Ramasamy, S. (2004). Geochemistry of sandstones from the Upper Miocene Kudankulam Formation, southern India: Implications for provenance, weathering and tectonic setting. *Journal of Sedimentary Research, 74*(2), 285–297. https://doi.org/10.1306/082803740285

Awasthi, N. (2017). Provenance and paleo–weathering of Tertiary accretionary prism–forearc sedimentary deposits of the Andaman Archipelago, India. *Journal of Asian Earth Sciences, 150*, 45–62. https://doi.org/10.1016/j.jseaes.2017.10.005

Basu, A., Young, S. W., Suttner, L. J., James, W. C., & Mack, G. H. (1975). Re-evaluation of the use of undulatory extinction and polycrystallinity in detrital quartz for provenance interpretation. *Journal of Sedimentary Petrology*, *45*, 873–882.

Bhakuni, S. S., Luirei, K., & Devi, M. (2012). Soft sediment deformation structures (seismites) in Middle Siwalik sediments of Arunachal Pradesh, NE Himalaya. *Himalayan Geology, 33*(2), 139–145.

Bhatia, M. R. (1985). Rare-earth element geochemistry of Australian Paleozoic graywackes and mudrocks: Provenance and tectonic control. *Sedimentary Geology, 45*, 97–113. https://doi.org/10.1016/0037-0738(85)90025-9

Bhatia, M. R., & Crook, K. A. (1986). Trace element characteristics of graywackes and tectonic setting discrimination of sedimentary basins. *Contribution to Mineralogy and Petrology, 92*, 181–193. https://doi.org/10.1007/BF00375292

Bhatia, M. R., & Taylor, S. R. (1981). Trace element geochemistry and sedimentary provinces: A study from the Tasman Geosyncline, Australia. *Chemical Geology, 33*, 115–126.

Bock, B., McLennan, S. M., & Hanson, G. N. (1998). Geochemistry and provenance of the middle Ordovician Austin glen member (Normanskill formation) and the Taconian Orogeny in new England. *Journal of Sedimentary Research, 45*, 635–655. https://doi.org/10.1046/j.1365-3091.1998.00168.x

Brookfield, M. E. (1993). The Himalayan passive margin from Precambrian to Cretaceous times. *Sedimentary Geology, 84*, 1–35. https://doi.org/10.1016/0037-0738(93)90042-4

Burchfiel, B. C., Chen, Z., Hodges, K. V., Liu, Y., Royden, L. H., Deng, C., & Xu, J. (1992). The South Tibet Detachment System, Himalayan orogen: Extension contemporaneous with and parallel to shortening in a collisional mountain belt. *Geological Society of America Special Paper, 269*, 1–41. https://doi.org/10.1086/376763

Burg, J. P., Brunel, M., Gapais, D., Chen, G. M., & Liu, G. H. (1984). Deformation of leucogranites of the crystalline main central sheet in southern Tibet (China). *Journal of Structural Geology, 6*, 535–542. https://doi.org/10.1016/0191-8141(84)90063-4

Catlos, E. J., Harrison, T. M., Kohn, M. J., Grove, M., Ryerson, F. J., Manning, C. E., & Upreti, B. N. (2001). Geochronologic and thermobarometric constraints on the evolution of the Main Central Thrust, central Nepal Himalaya. *Journal of Geophysical Research, 106*, 16177–16204.

Chauhan, D. S. (2015). Magmatic and geochemical evolution of Chirpatiyakhal and Thati Kathur granites, Kumaun Lesser Himalaya. Geological Survey of India Unpublished Report for F.S. 2013–2015, p. 118.

Chauhan, D. S., Chauhan, R., Shankar, B., & Kesari, G. K. (2022). Structural and Kinematic Study of Ghuttu Window: Implication on the Tectonic Evolution of Bhilangana Formation, Central Crystalline Group, Garhwal Himalaya, India. Journal of Earth System Sciences. (Accepted manuscript)

Chauhan, D. S., Shankar, B., & Chauhan, R. (2013). Tectonostratigraphy and tectonic setting of Bhilangana formation vis-à-vis Central crystallines. Geological Survey of India Unpublished Report for Field season 2010-2013, p. 117.

Clift, P. D., Hodges, K. V., Heslop, D., Hannigan, R., Van Long, H., & Calves, G. (2008). Correlation of Himalayan exhumation rates and Asian monsoon intensity. *Nature Geosciences, 1*, 875–880. https://doi.org/10.1038/ngeo351

Compton, R. R. (1962). *Manual of Field Geology* (p. 378). New York: John Wiley & Sons.

Cox, R., Lowe, D. R., & Cullers, R. L. (1995). The influence of sediment recycling and basement composition on evolution of mudrock chemistry in the southwestern United States. *Geochimica Et Cosmochimica Acta, 59*, 2919–2940. https://doi.org/10.1016/0016-7037(95)00185-9

Cullers, R. L. (1988). Mineralogical and chemical changes of soil and stream sediments formed by intense weathering of the Danberg granite, Georgia, USA. *Lithos, 21*, 301–314. https://doi.org/10.1016/0024-4937(88)90035-7

Cullers, R. L. (1994). The controls of major and trace elements variation of shales, siltstones and sandstones of Pennsylvanian-Permian age from uplifted continental blocks in Colorado to platform sediments in Kansas, USA. *Geochimica Et Cosmochimica Acta, 58*, 4955–4972. https://doi.org/10.1016/0016-7037(94)90224-0

Cullers, R. L. (2000). The geochemistry of shales, siltstones and sandstones of Pennsylvanian-Permian age, Colorado, USA: Implications for provenance and metamorphic studies. *Lithos, 51*, 181–203. https://doi.org/10.1016/S0024-4937(99)00063-8

Cullers, R. L., Basu, A., & Suttner, L. J. (1988). Geochemical signature of provenance in sandsize material in soil and stream sediments near the Tobbaco Root batholith, Montana, USA. *Chemical Geology, 70*, 335–348. https://doi.org/10.1016/0009-2541(88)90123-4

Cullers, R. L., & Graf, J. L. (1984). Rare earth elements in igneous rocks of the continental crust: intermediate and silicic rocks—ore petrogenesis. In P. Handerson (Ed.), *Rare earth element geochemistry* (pp. 275–316). Elsevier. https://doi.org/10.1016/B978-0-444-42148-7.50013-7

Das, B. N., Das, N., & Siddique, M. A. (1974). Reports on geological and geomorphological studies in parts of Sarda sub-basin Nainital and Pilibhit districts, U.P. Geological Survey of India Unpublished Report for Field Season 1973-1974, p. 24.

Das, B. P., Joshi, M., & Kumar, M. (2019). Tectonochemistry and P-T Conditions of Ramgarh and Almora Gneisses from Askot Klippe, Kumaun Lesser Himalaya. *Acta Geologica Sinica (English Edition), 93*(1), 1–11. https://doi.org/10.1111/1755-6724.13814

Debon, F., Le Fort, P., Sheppard, S. M. F., & Sonet, J. (1986). The four plutonic belts of the Transhimalaya-Himalaya: A chemical-mineralogical, isotopic and chronological synthesis along a Tibet-Nepal section. *Journal of Petrology, 27*(1), 219–250.

DeCelles, P. G., Gehrels, G. E., Quade, J., Ojha, T. P., Kapp, P. A., & Upreti, B. N. (1998). Neogene foreland basin deposits, erosional unroofing and the kinematic history of the Himalayan fold–thrust belt, western Nepal. *Geologcial Society of America Bulletin, 110*, 2–21. https://doi.org/10.1130/0016-7606(1998)110%3C0002:NFBDEU%3E2.3.CO;2

DeCelles, P. G., & Giles, K. A. (1996). Foreland basin systems. *Basin Research, 8*, 105–123. https://doi.org/10.1046/j.1365-2117.1996.01491.x

DeCelles, P. G., & Hertel, F. (1989). Petrology of fluvial sands from the Amazonian foreland basin, Peru and Bolivia. *Geologcial Society of America Bulletin, 101*(12), 1552–1562.

DeCelles, P. G., Robinson, D. M., Quade, J., Ojha, T. P., Garzione, C. N., Copeland, P., & Upreti, B. N. (2001). Stratigraphy, structure and tectonic evolution of the Himalayan fold–thrust belt in western Nepal. *Tectonics, 20*, 487–509. https://doi.org/10.1029/2000TC001226

Dickinson, W. R. (1985). Interpreting relations from detrital modes of sandstone. In G. G. Zuffa (Ed.), *Provenance of arenite* . Dordrecht-Boston-Lancaster, pp. 333–362.

Dickinson, W. R., & Suczek, C. A. (1979). Plate tectonics and sandstone compositions. *Bulletin of American Association of Petroleum Geology, 63*, 2164–2182. https://doi.org/10.1306/2F9188FB-16CE-11D7-8645000102C1865D

DiPietro, J. A., & Pogue, K. R. (2004). Tectonostratigraphic subdivisions of the Himalaya: A view from the west. *Tectonics, 23*(5), 1–20. https://doi.org/10.1029/2003TC001554

Fedo, C. M., Eriksson, K. A., & Krogstad, E. J. (1996). Geochemistry of shales from the Archean (~3.0 Ga) Buhwa Greenstone Belt, Zimbabwe: Implications for provenance and source-area weathering. *Geochimica Et Cosmochimica Acta, 60*, 1751–1763. https://doi.org/10.1016/0016-7037(96)00058-0

Fedo, C. M., Nesbitt, H. W., & Young, G. M. (1995). Unraveling the effects of potassium metasomatism in sedimentary rocks and paleosols, with implications for paleoweathering conditions and provenance. *Geology, 23*, 921–924. https://doi.org/10.1130/0091-7613(1995)023%3c0921:UTEOPM%3e2.3.CO;2

Floyd, P. A., & Leveridge, B. E. (1987). Tectonic environment of the Devonian Gramscatho Basin South Cornwall: Framework Mode and Geochemical Evidence from Turbiditic Sandstones. *Journal of the Geological Society (London), 144*, 531–542. https://doi.org/10.1144/gsjgs.144.4.0531

Folk, R. L. (1974). *Petrology of sedimentary rocks* (p. 182). Hemphill Publishing Co.

Folk, R. L. (1980). *Petrology of sedimentary rocks* (p. 182). Hemphill.
Frank, W., Thoni, M., & Purtscheller, F. (1977). Geology and petrography of Kulu-south Lahul area. *Himalayas* (Vol. 268, pp. 147–172). Science de la Terre, CNRS.
Fuchs, G., & Linner, M. (1995). Geological traverse across the western Himalaya—a contribution to the geology of eastern Ladakh, Lahul, and Chamba. *Jahrbuch Der Geologischen Bundesanstalt., 138*, 665–685.
Gallet, S., Jahn, B., Van Vliet Lanoe, B., Dia, A., & Rossello, E. (1998). Loess geochemistry and its implications for particle origin and composition of the upper continental crust. *Earth and Planetary Science Letters, 156*, 157–172. https://doi.org/10.1016/S0012-821X(97)00218-5
Ganesan, T. M. (1975). Paleocurrent pattern in the Upper Tal rocks of Nigali, Korgai Synclies (H.P.) and Mussoori Syncline (U.P.). *Journal of Geological Society of India, 16*, 503–507.
Gansser, A. (1964). *Geology of the Himalayas* (p. 289). Wiley InterScience.
Garcia, D., Fonteilles, M., & Moutte, J. (1994). Sedimentary fractionations between Al, Ti, and Zr and the genesis of strongly peraluminous granites. *Journal of Geology, 102*, 411–422. https://doi.org/10.1086/629683
Ghosh, S. K., & Kumar, R. (2000). Petrography of Neogene Siwalik Sandstone of the Himalayan Foreland Basin, Garhwal Himalaya: Implications for Source-Area Tectonics and Climate. *Journal of Geological Society of India, 55*(1), 1–15.
Ghosh, S. K., Kumar, R., & Suresh, N. (2003). Influence of Mio-Pliocene drainage re-organisation in the detrital modes of sandstone, Subathu sub-basin, Himalayan Foreland Basin. *Himalayan Geology, 24*(1), 35–46.
Harrison, T. M., Lovera, O. M., & Grove, M. (1997). New insights into the origin of two contrasting Himalayan granite belts. *Geology, 25*, 899–902. https://doi.org/10.1130/0091-7613(1997)025%3c0899:NIITOO%3e2.3.CO;2
Hayashi, K. I., Fujisawa, H., Holland, H. D., & Ohmoto, H. (1997). Geochemistry of 1.9 Ga sedimentary rocks from northeastern Labrador. *Canada. Geochimica Et Cosmochimica Acta, 61*, 4115–4137. https://doi.org/10.1016/s0016-7037(97)00214-7
Heim, A., & Gansser, A. (1939). *Central Himalaya: Geological observations of the Swiss expedition 1936* (p. 246). Gebruder Fretz.
Herron, M. M. (1988). Geochemical classification of terrigenous sands and shales from core of log data. *Journal of Sedimentary Petrology, 58*, 820–829.
Hussain, F. M., & Bharali, B. (2019). Whole-rock geochemistry of Tertiary sediments of Mizoram Foreland basin, NE India: Implications for source composition, tectonic setting and sedimentary processes. *Acta Geochim, 38*(6), 897–914. https://doi.org/10.1007/s11631-019-00315-3
Huyghe, P., Galy, A., Mugnier, J. L., & France-Lanord, C. (2001). Propagation of the thrust system and erosion in the Lesser Himalaya: Geochemical and sedimentological evidence. *Geology, 29*, 1007–1010. https://doi.org/10.1130/0091-7613(2001)029%3c1007:POTTSA%3e2.0.CO;2
Ingersoll, R. V., & Suczek, C. A. (1979). Petrology and provenance of Neogene sand from Nicobar and Bengal fans, DSDP sites 211 and 218. *Journal of Sedimentary Petrology, 49*, 1217–1228. https://doi.org/10.1306/212F78F1-2B24-11D7-8648000102C1865D
Islam, R., Ahmad, T., & Khanna, P. P. (2005). An overview on the granitoids of the NW Himalaya. *Himalayan Geology, 26*(1), 49–60.
Jayangondaperumal, R., Thakur, V. C., Joevivek, V., Priyanka, R. S., & Gupta, A. K. (2018). *Active tectonics of Kumaun and Garhwal Himalaya* (p. 150). Springer.
Khan, T., Srinivasa Sarma, D., & Shamim Khan, M. (2020). Geochemical study of the Neoproterozoic clastic sedimentary rocks of the Khambal Formation (Sindreth Basin), Aravalli Craton, NW Indian Shield: Implications for paleoweathering, provenance, and geodynamic evolution. *Geochemistry, 80*, 125596. https://doi.org/10.1016/j.chemer.2019.125596
Khan, T., Srinivasa Sarma, D., Somasekhar, V., Ramaniah, S., & Ramakrishna Reddy, N. (2019). Geochemistry of the Palaeoproterozoic quartzites of Lower Cuddapah Supergroup, South India: Implications for the palaeoweathering, provenance, and crustal evolution. *Geological Journal, 2019*, 1–25. https://doi.org/10.1002/gj.3489
Khanna, P. P., Saini, N. K., Mukherjee, P. K., & Purohit, K. K. (2009). An appraisal for ICP-MS technique for determination of REEs: Long term QC assessment of silicate rock analysis. *Himalayan Geology, 30*(1), 95–99.
Kohn, M. J., Paul, S. K., & Corrie, S. L. (2010). The lower Lesser Himalayan sequence: A Paleoproterozoic arc on the northern margin of the Indian plate. *Geological Society of America Bulletin, 122*(3–4), 323–335. https://doi.org/10.1130/b26587.1
Krynine, P. D. (1940). *Petrology and genesis of the third Bradford sand* (Vol. 29, p. 134). Pennsylvania Statistic College.
Kumar, R., Ghosh, S. K., Sangode, S. J., & Phadtare, N. R. (1999). Evolution of the Plio-Pleistocene contrasting alluvial fans in the Siwalik Foreland Basin, NW Himalaya, India. In A. K. Jain & R. Manickavasagam (Eds.), *Geodynamics of the NW Himalaya* (Vol. 6, pp. 296–304). Gondvana Research Group Memoirs.
Kumar, R., & Kotiyal, P. L. (1993). Quaternary Geology and Geoomorphology of Pilibhit-Khatima area of Ganga Basin in parts of Bareilly, Nainital and Pilibhit District, Uttar Pradesh. Unpublished Report Geological Survey of India Field Season 1992-1993, p. 54.
LeFort, P. (1975). Himalayas—collided range—present knowledge of continental arc. *American Journal of Sciences, A275*, 1–44.
LeFort, P. (1988). Granite in the tectonic evolution of Himalaya, Karakoram and southern Tibet. Tectonic evolution of the Himalayas and Tibet. *Philosophical Transactions of Royal Society, London, 326*, 281–299. https://doi.org/10.1098/rsta.1988.0088
LeFort, P. (1996). Evolution of the Himalaya. In A. Yin & T. M. Harrison (Eds.), *The tectonics of Asia* (pp. 95–106). Cambridge University Press.
Lucas-Tooth, H. J., & Pyne, C. (1964). The accurate determination of major constituents by X-ray fluorescent analysis in the presence of large interelement effects. *Advances in X-ray Analysis, 7*, 523–541.
Macfarlane, A. M., Hodges, K. V., & Lux, D. (1992). A structural analysis of the Main Central Thrust zone, Langtang National Park, central Nepal Himalaya. *Geological Society of America Bulletin, 104*(11), 1389–1402. https://doi.org/10.1130/0016-7606(1992)104%3c1389:ASAOTM%3e2.3.CO;2
Mack, G. H., & Suttner, L. J. (1977). Paleoclimate interpretation from petrographic comparison of Holocene sands and the Fountain Formation (Pennsylvanian) in the Colorado Front Range. *Journal of Sedimentary Petrology, 47*, 89–100.
Mandal, S. K., Scherler, D., Romer, R. L., Burg, J., Guillong, M., & Schleicher, A. M. (2018). Multiproxy Isotopic and geochemical analysis of the Siwalik sediments in NW India: Implication for the late Cenozoic tectonic evolution of the Himalaya. *Tectonics, 38*, 120–143. https://doi.org/10.1029/2018TC005200
Maynard, J. B., Valloni, R., & Yu, H. S. (1982). *In sedimentation and tectonics on modern and ancient active plate margins* (pp. 551–561). Blackwell Scientific.
McLennan, S. M. (1989). Rare earth elements in sedimentary rocks: Influence of provenance and sedimentary processes. *Geochemistry and Mineralogy of Rare Earth Elements Reviews Mineralogy, 21*, 169–200. https://doi.org/10.1515/9781501509032-010
McLennan, S. M. (2001). Relationship between trace element composition of sedimentary rocks and upper continental crust.

Geochemistry, Geophysics, Geosystems. https://doi.org/10.1029/2000GC000109
McLennan, S. M., Hemming, S., McDaniel, D. K., & Hanson, G. N. (1993). Geochemical approaches to sedimentation, provenance and tectonics. *Geological Society of America Special Paper, 284*, 295–303. https://doi.org/10.1130/SPE284-p21
McLennan, S. M., Nance, W. B., & Taylor, S. R. (1980). Rare earth element-thorium correlations in sedimentary rocks, and the composition of the continental crust. *Geochimica Et Cosmochimica Acta, 44*(11), 1833–1839. https://doi.org/10.1016/0016-7037(80)90232-X
Mehta, J. S. (1993). Final report on I and S granites of Almora, Binsar, Mukteshwar, Champawat, Ramgarh and Amritpur Area, Almora, Pithoragarh and Nainital districts, U.P. Geological Survey of.India Unpublished Report for F.S. 1988–93, p. 101.
Miall, A. D. (1996). *The geology of fluvial deposits* (p. 582). Springer.
Myrow, P. M., Hughes, N. C., Paulsen, T., Williams, I., Parcha, S. K., Thompson, K. R., Bowring, S. A., Peng, S.-C., & Ahluwalia, A. D. (2003). Integrated tectonostratigraphic analysis of the Himalaya and implications for its tectonic reconstruction. *Earth and Planetary Science Letters, 212*, 433–441. https://doi.org/10.1016/S0012-821X(03)00280-2
Najman, Y. (1995). Evolution of the early Himalayan foreland basin in NW India and its relationship to Himalayan orogenesis. PhD Thesis. Edinburgh University, 1–307.
Najman, Y. (2006). The detrital record of orogenesis: A review of approaches and techniques used in the Himalayan sedimentary basins. *Earth Science Review, 74*, 1–72. https://doi.org/10.1016/j.earscirev.2005.04.004
Najman, Y., & Garzanti, E. (2000). An integrated approach to provenance studies: Reconstructing early Himalayan paleogeography and tectonic evolution from Tertiary foredeep sediments, N. India. *Geological Society of America Bulletin, 112*, 435–449.
Nakamura, N. (1974). Determination of REE, Ba, Fe, Mg, Na and K in carbonaceous and ordinary chondrites. *Geochimica Et Cosmochimica Acta, 38*, 757–775. https://doi.org/10.1016/0016-7037(74)90149-5
Nance, W. B., & Taylor, S. R. (1976). Rare earth element pattern and crustal evolution: I. Australian post-Archean sedimentary rocks. *Geochimica Et Cosmochimica Acta, 40*, 1539–1551. https://doi.org/10.1016/0016-7037(76)90093-4
Nesbitt, H. W., Markovics, G., & Price, R. C. (1980). Chemical processes affecting alkalis and alkaline earths during continental weathering. *Geochimica Et Cosmochimica Acta, 44*(11), 1659–1666. https://doi.org/10.1016/0016-7037(80)90218-5
Nesbitt, H. W., & Young, G. M. (1984). Prediction of some weathering trends of plutonic and volcanic rocks based on thermodynamic and kinetic considerations. *Geochimica Et Cosmochimica Acta, 48*, 1523–1534. https://doi.org/10.1016/0016-7037(84)90408-3
Nockolds, S. R., & Allen, R. (1956). The geochemistry of some igneous rock series-III. *Geochimica Et Cosmochimica Acta, 9*, 34–77. https://doi.org/10.1016/0016-7037(56)90056-4
Palmer, H. S. (1916). Nomographic solutions of certain stratigraphic measurements. *Economic Geology*, *11*, 14–29.
Passchier, C. W., & Trouw, R. A. J. (1995). *Microtectonics*. Springer-Verleg.
Pettijohn, F. J., Potter, P. E., & Siever, R. (1973). *Sand and sandstone* (p. 618). Springer-Verlag.
Potter, P. E., Maynard, J. B., & Depetris, P. J. (2005). *Mud and mudstones* (p. 297). Springer.
Raina, B. N. & Dungrakoti, B. D. (1965). Report on the study of Bhowali Traps of U.P. Himalaya. Unpublished Report Geological Survey of India Field Season 1964–1965, p. 42.
Ranjan, N., & Banerjee, D. M. (2009). Central Himalayan crystallines as the primary source for the sandstone-mudstone suites of the Siwalik Group: New geochemical evidence. *Gondwana Research, 16*, 687–696. https://doi.org/10.1016/j.gr.2009.07.005
Rao, D. R., & Sharma, R. (2009). Petrogenesis of the granitoid rocks from Askot Crystallines Kumaun Himalaya. *Journal of Geological Society of India, 73*, 553–566.
Rao, D. R., & Sharma, R. (2011). Arc magmatism in eastern Kumaun Himalaya, India: A study based on geochemistry of granitoid rocks. *Island Arc, 20*, 500–519. https://doi.org/10.1111/j.1440-1738.2011.00781.x
Roddaz, M., Baby, P., Brusset, S., Hermoza, W., & Darrozes, J. M. (2005). Forebulge dynamics and environmental control in Western Amazonia: The case study of the Arch of Iquitos (Peru). *Tectonophysics, 399*, 87–108.
Roddaz, M., Viers, J., Brusset, S., Baby, P., Boucayrand, C., & Herail, G. (2006). Controls on weathering and provenance in the Amazonian foreland basin: Insights from major and trace element geochemistry of Neogene Amazonian sediments. *Chemical Geology, 226*, 31–65.
Rollinson, H. (1993). *Using geochemical data: Evaluation, presentation, interpretation* (p. 352). Longman Scientific and Technical.
Roser, B. P., & Korsch, R. J. (1986). Determination of tectonic setting of sandstone-mudstone suits using SiO_2 and K_2O/Na_2O ratio. *Journal of Geology, 94*, 635–650. https://doi.org/10.1086/629071
Roser, B. P., & Korsch, R. J. (1999). Geochemical characterization, evolution and source of a Mesozoic accretionary wedge: The Torlesse terrane, New Zealand. *Geological Magazine, 136*(5), 493–512. https://doi.org/10.1017/S0016756899003003
Roy, D. K., & Roser, B. P. (2013). Geochemical evolution of the Tertiary succession of the NW shelf, Bengal basin, Bangladesh: Implications for provenance, paleoweathering and Himalayan erosion. *Journal of Asian Earth Sciences, 78*, 248–262. https://doi.org/10.1016/j.jseaes.2013.04.045
Sawant, S. S., Vijay Kumar, K., Balaram, V., Subba Rao, D. B., Rao, K. S., & Tewari, R. P. (2017). Geochemistry and genesis of craton-derived sediments from active continental margins: Insights from the Mizoram Foreland basin, NE India. *Chemical Geology, 470*, 13–32.
Saxena, A. (1975). Geology of parts of Champawat Tehsil, District Pithoragarh, U.P. Unpublisehd Report Geological Survey of India Field Season 1974–75, p. 28.
Saxena, A. (1978). Geology of the area in parts of Champawat Tehsil, District Pithoragarh, Uttar Pradesh. Unpublisehd Report Geological Survey of India Field Season 1977–78, p. 24.
Schwab, F. L. (1986). Sedimentary 'signatures' of foreland basin assemblages: Real or counterfeit? In P. A. Allen & P. Homewood (Eds.), *Foreland Basins* (Vol. 8, pp. 395–410). Special Publicaiton of International Association of Sedimentologist.
Searle, M. P., Law, R. D., Godin, L., Larson, K., Streule, M. J., Cottle, J. M., & Jessup, M. J. (2008). Defining the Himalayan Main Central Thrust in Nepal. *Journal of Geological Society, London, 165*, 523–534.
Sharma, R., Gupta, V., Arora, B. R., & Sen, K. (2011). Petrophysical properties of the Himalayan granitoids: Implication on composition and source. *Tectonophysics, 497*, 23–33. https://doi.org/10.1016/j.tecto.2010.10.016
Singh, G. & Kothiyal, P. L. (1997). Quaternary geological and geomorphological studies in parts of Ramganga (East) Sub basin of Kali basin, Pithoragarh District, Uttar Pradesh. Geological Survey of India Unpublished Report. for field season 1996–1997.
Sinha, S., Ghosh, S. K., Kumar, R., Islam, R., Sanyal, P., & Sangode, S. J. (2008). Role of tectono-climatic factors in the Neogene Himalayan Foreland sediments: Petrology and geochemical approach, Kangra Sub-basin. *Journal of Geological Society of India, 71*, 787–807.

Sinha, S., Islam, R., Ghosh, S. K., Kumar, R., & Sangode, S. J. (2007). Geochemistry of Neogene Siwalik mudstones along Punjab re-entrant, India: Implications for source-area weathering, provenance and tectonic setting. *Current Science, 92*(8), 1103–1113.

Sinha, S., Sangode, S. J., Kumar, R., & Ghosh, S. K. (2005). Accumulation history and tectonic significance of the Neogene continental deposits in the west central sector of the Himalayan foreland basin. *Himalayan Geology, 26*(2), 387–408.

Tandon, S. K., & Varshney, S. K. (1991). Origin of selective carbonate cemented (concretionary) layers within multistoried sandstone bodies of the Neogene Middle Siwalik Subgroup, NW Himalaya, India. Abstract, Birbal Sahni Birth Centenary Symposium on the Siwalik Basin, WIHG, Dehra Dun, India, 45.

Taylor, S. R. (1964). Abundance of chemical elements in the continental crust: A new table. *Geochimica Et Cosmochimica Acta, 28*(8), 1273–1285. https://doi.org/10.1016/0016-7037(64)90129-2

Taylor, S. R., & McLennan, S. M. (1985). *The continental crust: its composition and evolution* (p. 312). Blackwell.

Taylor, S. R., & McLennan, S. M. (1995). The geochemical evolution of the continental crust. *Reviews of Geophysics, 33*(2), 241–265. https://doi.org/10.1029/95RG00262

Thakur, V. C. (1992). *Geology of Western Himalaya* (p. 363). Pergamon Press.

Thakur, V. C. (2013). Active tectonics of Himalayan frontal fault system. *International Journal of Earth Science (Geol Rundsch), 102*, 1791–1810. https://doi.org/10.1007/s00531-013-0891-7

Turekian, K. T. (1963). The chromium and nickel distribution in basaltic rocks and eclogites. *Geochimica Et Cosmochimica Acta, 27*, 835–846. https://doi.org/10.1016/0016-7037(63)90046-2

Ulak, P. D., Roser, B., & Zakir Hossain, H. M. (2008). Major and trace element analyses of sandstones and mudstones from the Siwalik Group, Bakiya Khola, central Nepal. *Geoscience Reports, Shimane University, 27*, 43–51.

Valdiya, K. S. (1970). Simla slates: The Precambrian Flysch of the Lesser Himalaya, its turbidites, sedimentary structures and paleocurrents. *Geological Society of America Bulletin, 81*(2), 451–468.

Valdiya, K. S. (1980). *Geology of Kumaun Lesser Himalaya* (p. 289). Wadia Institute of Himalayan Geology.

Valdiya, K. S. (1999). Rising Himalaya: Advent and intensification of monsoon. *Current Science, 76*(4), 514–524.

Van Der Beek, P., Robert, X., Mugnier, J. L., Bernet, M., Huyghe, P., & Labrin, E. (2006). Late Miocene—recent exhumation of the central Himalaya and recycling in the foreland basin assessed by apatite fission-track thermochronology of Siwalik sediments, Nepal. *Basin Research, 18*, 413–434. https://doi.org/10.1111/j.1365-2117.2006.00305.x

Vinogradov, A. P. (1962). Average contents of chemical elements in the major types of terrestrial igneous rocks. *Geokhimiya, 7*, 555–571.

Visser, J. N. J., & Young, G. M. (1990). Major element geochemistry and paleoclimatology of the Permo-Carboniferous glacigene Dwyka Formation and postglacial mudrocks in southern Africa. *Palaeogeography Palaeoclimatology Palaeoecology, 81*(1–2), 49–57. https://doi.org/10.1016/0031-0182(90)90039-a

Wesnousky, S. G., Kumar, S., Mohindra, R., & Thakur, V. C. (1999). Uplift and convergence along the Himalayan frontal thrust of India. *Tectonics, 18*(6), 967–976. https://doi.org/10.1029/1999TC900026

Whitney, D. N., & Evans, B. W. (2010). Abbreviations of names of rock forming minerals. *American Mineralogist, 95*, 185–187. https://doi.org/10.2138/AM.2010.3371

Willis, K. M., Stern, R. J., & Clauer, N. (1988). Age and geochemistry of Late Precambrian sediments of the Hammamat Series from the Northeastern Desert of Egypt. *Precambrian Research, 42*, 173–187. https://doi.org/10.1016/0301-9268(88)90016-2

Wronkiewicz, D. J., & Condie, K. C. (1987). Geochemistry of Archean shales from the Witwatersrand Supergroup, South Africa: Source-area weathering and provenance. *Geochimica Et Cosmochimica Acta, 51*, 2401–2416. https://doi.org/10.1016/0016-7037(87)90293-6

Yin, A. (2006). Cenozoic tectonic evolution of the Himalayan orogen as constrained by along-strike variation of structural geometry, exhumation history, and foreland sedimentation. *Earth Science Review, 76*, 1–131. https://doi.org/10.1016/j.earscirev.2005.05.004

Zachos, J., Pagani, M., Sloan, L., Thomas, E., & Billups, K. (2001). Trends, rhythms and aberrations in global climate 65 Ma to present. *Science, 292*, 686–693. https://doi.org/10.1126/science.1059412